olefin of Tam are crucial for ER binding activity.[13] So, we considered that more symmetrical derivatives of Tam might show reduced ER-binding ability.

Among our synthesized compounds, we found two, compounds **1** (YAK01) and **3** (YAK037), with potent L-Glu transporter-inhibitory activity. Studies of their mechanisms of action indicated that, unlike Tam, compound **3** acts through an ER-independent and MAPK-independent, but PI3K-dependent pathway and shows no transactivation activity for nERs. We believe this compound may represent a new platform for developing novel L-Glu transporter inhibitors with higher brain transfer rates and reduced adverse effects.

■ RESULTS AND DISCUSSION

We synthesized several Tam-inspired compounds bearing identical substituents on one carbon atom of the olefin,[12] and found that two of them were potent inhibitors of astrocyte L-Glu transporters. The diethyl-substituted derivative **1** inhibited L-Glu transporters in the picomolar range (62.7 ± 7.48% of control at 1 pM; Figure 2A). The dose–response curve for the inhibitory activity was not linear, but followed an inverted U-shaped curve; however, such a non-monotonic dose dependence is rather common for hormones and their mimetics.[14] On the other hand, when the symmetrical substituent was changed from ethyl to benzyl (**2**), the inhibitory effect was lost (Figure 2B). However, when the phenolic oxygen atom of **1** was substituted with a *N*,*N*-dimethylaminoethyl group (Figure 1C), we found

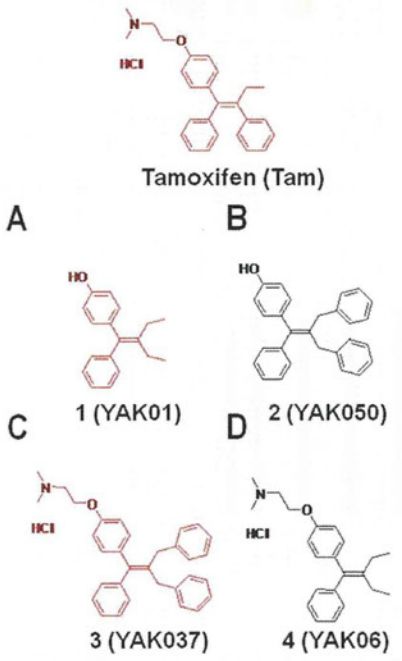

Figure 1. Chemical structures of the newly synthesized tamoxifen-related compounds.

that the resulting compound **3** showed dose-dependent L-Glu transporter inhibition in the picomolar range (63.8 ± 5.49% of control at 1 pM; Figure 2C). The dose-dependency of the effect of **3** suggested that the underlying mechanism might be different from that in the case of **1**. Compound **4** was inactive (Figure 2D).

We next examined the effects of **1** and **3** on cell viability by means of MTT reduction assay and LDH leakage assay, using the same cultured sample. Neither of the compounds was cytotoxic at concentrations below 1 μM (Figure 3), though 100 μM **1** and 10 μM **3** caused severe cell damage. These results exclude the possibility that the L-Glu clearance-inhibitory effects of these compounds at concentrations below 1 μM were caused by cell damage.

In order to confirm the involvement of L-Glu transporters in the inhibition of L-Glu uptake by our compounds, and to rule out the possibility that **1** and **3** act by inducing L-Glu release from astrocytes, we next examined the effect of **1** and **3** on L-Glu clearance when the L-Glu transporter activity was blocked with TBOA, a potent nonselective L-Glu transporter inhibitor (IC_{50}: 48 μM for GLAST/EAAT1, 7 μM for GLT1/EAAT2). We confirmed that application of 1 mM TBOA potently inhibited L-Glu transporter activity; that is, TBOA caused reversible chemical knock-down of L-Glu transporter activity.[7] When either **1** or **3** was coapplied with 1 mM TBOA, these compounds no longer influenced L-Glu clearance (Figure 4), indicating that the actions of these compounds are indeed mediated by L-Glu transporters, and do not involve L-Glu release from astrocytes.

Our cultured astrocytes predominantly expressed ERα, and little or no expression of ERβ was detected.[5] Tam is known to be a partial agonist of ERs,[9] raising the possibility that the compounds exerted their inhibitory effects via interaction with ERα. Therefore, we examined the involvement of ERα by coapplication of ICI182,780, a high-affinity antagonist of ERs. ICI182,780 dose-dependently blocked the inhibition of L-Glu uptake caused by **1** (Figure 5A) at 0.01, 0.1, and 1 μM, at which the effects of Tam were reported to be completely suppressed.[7] In contrast, ICI182,780 had no effect on the inhibition by **3** (Figure 5B), suggesting that the mechanism of the inhibition by **3** is independent of ERs. We further examined the signal transduction pathways mediating the effects of **1** and **3**. When coapplied with U0126, which inhibits mitogen-activated protein kinase/extracellular signal-regulated kinase 1 (MEK1, IC50: 70 nM) and MEK2 (IC50: 60 nM), the inhibitory effect by **1** was blocked, whereas that of **3** was not (Figure 6A). On the other hand, when coapplied with LY294002, a specific phosphoinositide 3-kinase (PI3K) inhibitor (IC50: 70 nM), the inhibitory effects of both compounds were completely blocked (Figure 6B). These results suggest that PI3K is a common mediator of the effects of both compounds, whereas mitogen-activated protein kinase (MAPK) is involved only in the mechanism of inhibition by **1**.

Finally we examined the ER-agonist potency of **1** and **3**, i.e., the transcriptional effects of these compounds via human ERα and ERβ, using HEK293/hERα and HEK293/hERβ reporter cells (Figure 7). Compound **1** showed agonist activity in both of 293/hERα and 293/hERβ reporter cells, though the binding affinities were much weaker than that of E2. The EC50 values of **1** for ERα and ERβ are 30.8 nM and 10.4 nM, respectively (1.25 nM and 0.864 nM, respectively, for E2). The relative agonist activity of **1** was 66.8% of that of E2 in HEK293/hERα and 122.0% of that of E2 in HEK293/hERβ. Strikingly, **3** showed no agonist potency for ERα or ERβ. These findings strongly suggest that **3** can inhibit L-Glu transporters without interaction with ERs.

In this study, we examined the potential of Tam-related compounds to inhibit GLAST/EAAT1 and GLT1/EAAT2, which are major astrocytic L-Glu transporters in the rat

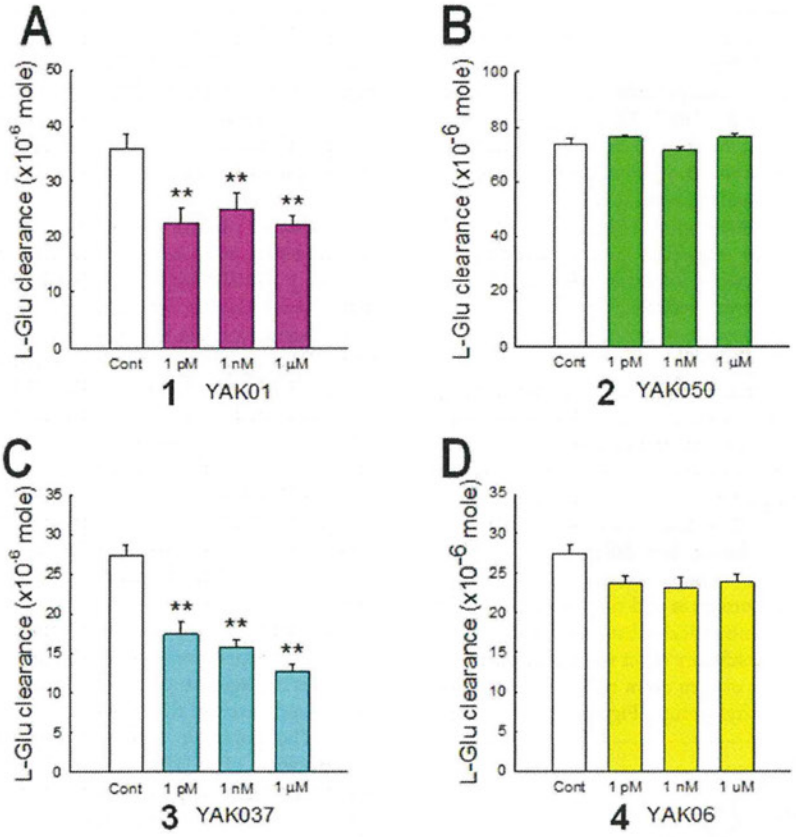

Figure 2. Compounds **1** and **3** inhibited L-Glu clearance in cultured astrocytes. The open column shows the control clearance, and colored columns show the clearance in the presence of various concentrations of compounds **1** (A), **2** (B), **3** (C), and **4** (D). $^{**}p < 0.01$ vs control group ($N = 6$), Tukey's test following ANOVA.

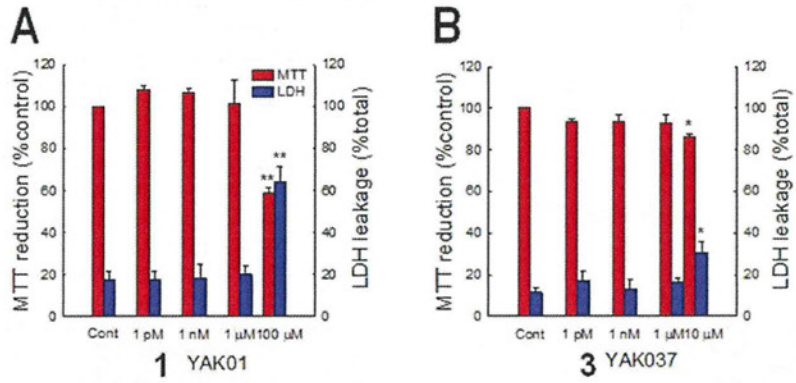

Figure 3. Effects of compounds **1** and **3** on cell viability. The results of MTT reduction and LDH leakage assays of **1** (A) and **3** (B) are shown. $^{*}p < 0.05$, $^{**}p < 0.01$ vs control group ($N = 6$), Tukey's test following ANOVA.

forebrain. Although GLT-1 is the main regulator of synaptically released L-Glu in vivo, the predominant subtype changes to GLAST in cultured astrocytes, possibly owing to the lack of interaction of astrocytes with neurons.[15] We confirmed that GLAST is the main functional L-Glu transporter in our primary-cultured astrocytes by Western blotting and pharmacological experiments (data not shown), in accordance with a previous report.[16] Therefore, the effects of the compounds observed here can be interpreted as being due to modulation of GLAST functional activity.

There is growing evidence that ERα, which is a nER that mediates genomic effects, can also be translocated to plasma membranes and mediate acute nongenomic effects in some cases. Transfection of CHO cells with nERs was reported to result in ER expression in both nuclei and membranes.[17] ERs on the plasma membranes of tumor cells were demonstrated to be structurally similar to nERs.[18] Further, mERα activated metabotropic glutamate receptor 5 (mGluR5) in striatal neurons in the CNS.[19] In our previous study, we clarified that the predominant ER subtype in cultured astrocytes was ERα, and

dx.doi.org/10.1021/cn200091w | ACS Chem. Neurosci. 2012, 3, 105–113

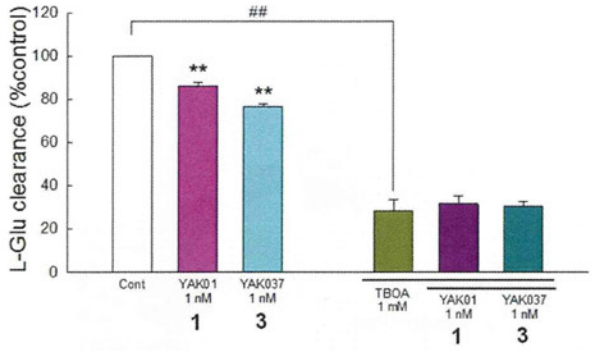

Figure 4. Compounds **1** and **3** suppressed L-Glu clearance in astrocyte culture by decreasing the functional activity of L-Glu transporter. L-Glu clearance in the presence and absence of compounds **1** and **3** is shown, together with their effects in the copresence of the potent nonselective L-Glu transporter inhibitor TBOA. $^{**}p < 0.01$ vs control group ($N = 6$), Tukey's test following ANOVA.

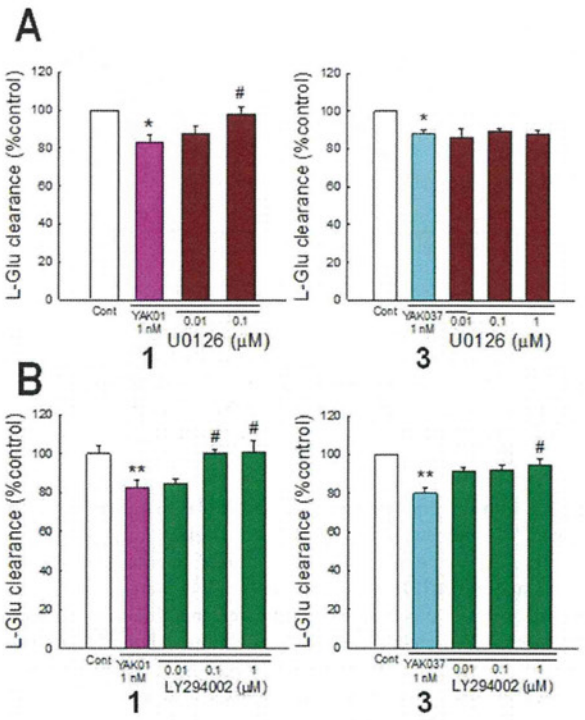

Figure 6. Involvement of MAPK and PI3K in the L-Glu transporter-inhibitory activity of compounds **1** (A) and **3** (B). Effects of compounds **1** (left panels) and **3** (right panels) on L-Glu clearance in the presence and absence of various concentrations of U0126, an inhibitor of MAPK/ERKs (A) or LY294002, a specific inhibitor of PI3K (B). $^{*}P < 0.05$, $^{**}p < 0.01$ vs control group, $\#p < 0.05$ vs compound-treated group ($N = 6$), Tukey's test following ANOVA.

estrogens (such as E2 and Tam) inhibited L-Glu transporter activity via the activation of mERα.[5] We found that the effects of **1** were blocked by ICI182,780, suggesting an interaction of **1** with ERα. In addition, our pharmacological experiments showed that activation of both of MAPK and PI3K is necessary for the L-Glu transporter-inhibitory activity of **1**. There are many reports indicating that nongenomic effects involving mERα are mediated via MAPK[19−21] and PI3K.[20,22] Taken together, the effects of **1** may be mediated by mERα in a similar manner to E2 and Tam. E2 was reported to activate MAPK via both PI3K-dependent and independent pathways in a single neuron.[20] Whether or not the same signaling pathways also exist in astrocytes is not yet known. It is of interest that other studies have found that estrogens also inhibit dopamine transporter (DAT) through the activation of mERα.[23,24]

On the other hand, the effect of **3** was ER-independent and MAPK-independent, but PI3K-dependent. Our binding assay revealed that **1** binds with ERs, but **3** does not. Based on these results, we propose that the mechanisms of the L-Glu transporter-inhibitory effects of **1** and **3** are different, as illustrated in Figure 8. The effect of **3** was possibly mediated by GPR30, a newly found ER, which is suggested to mediate the rapid nongenomic effects of estrogens.[25,26] In the case of GPR30, ICI182,780 acts as agonist, leading to activation of

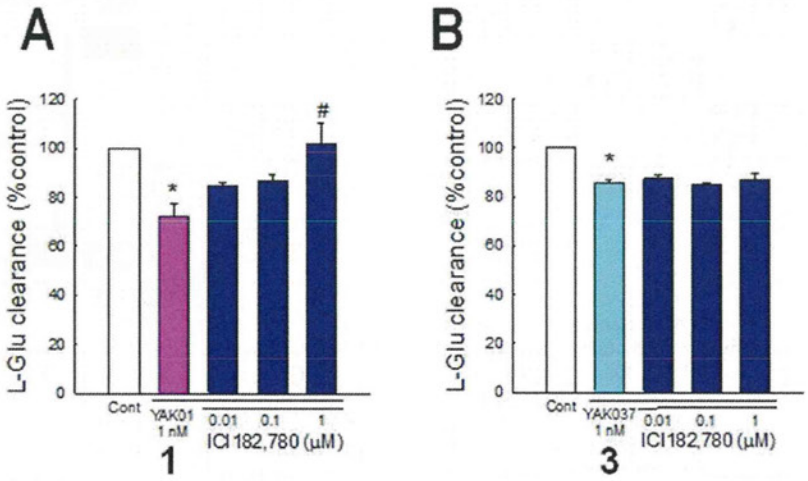

Figure 5. Involvement of ERs in the L-Glu transporter-inhibitory effects of compounds **1** and **3**. Effects of compounds **1** (A) and **3** (B) on L-Glu clearance in the presence and absence of various concentrations of ICI182,780, a high-affinity antagonist of ERs. $^{*}P < 0.05$ vs control group, $\#p < 0.05$ vs compound-treated group ($N = 6$), Tukey's test following ANOVA.

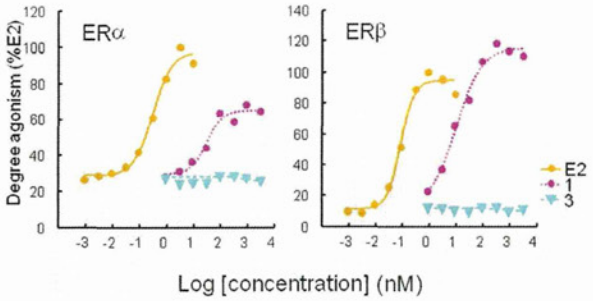

Figure 7. ER agonist potency of compounds **1** and **3** to nERs: dose dependence of binding of compounds **1** and **3** in HEK293/hERα cells (left) or HEK293/hERβ cells (right). Compound 1 showed dose-dependent agonist activity in both of HEK293/hERα cells (left) and HEK293/hERβ cells (right), though 3 showed no agonist potency for ERα or ERβ.

signal transduction pathways in a similar manner to estrogens.[27,28] However, we could not detect any effects of ICI182,780 alone on L-Glu transporter in our experiments (data not shown). In addition, Kuo et al. reported that GPR30 in astrocytes is detected not in the cell membranes but in the smooth endoplasmic reticulum,[29] while the cellular localization of GPR30 has been still controversially argued. In these contexts, GPR30 is an unlikely mediator to block the L-Glu transporters by the action of **3**.

According to Kisanga et al., the concentration of Tam in serum during conventional treatment for breast cancer (1−20 mg daily) is in the range from 20 to 225 nM.[30] Because **3** is more hydrophobic than Tam (the values of clogP for Tam and **3** are 7.56 and 9.70, respectively), it should exhibit greater permeability into the brain. Although other L-Glu transporter inhibitors, mainly L-Glu/aspartate analogues, are known, few of them have high brain transfer rates. Therefore, **3** is expected to be useful for biological research, and is also considered to be a promising candidate or lead compound for pharmacological application.

In conclusion, examination of several Tam-inspired compounds led to the discovery of two compounds that inhibited astrocytic L-Glu transporters at picomolar concentration. The inhibitory activity of compound **1** was mediated through the ER-MAPK/PI3K pathway, like that of Tam, though its transactivation activity was drastically reduced as compared with E2. In contrast, the inhibitory effect of **3** was manifested through an ER-independent and MAPK-independent, but PI3K-dependent pathway, and **3** showed no transactivation activity. These results suggest that **3** may represent a new platform for the development of novel L-Glu transporter inhibitors with higher brain transfer rates and reduced adverse effects.

METHODS

Chemistry. *General Procedures.* All reagents were commercial products and were used without further purification, unless otherwise noted. NMR data were recorded on a JEOL-400 or a Bruker Avance 400 NMR spectrometer (400 MHz for ^{1}H NMR and 100 MHz for ^{13}C NMR). *d*-$CDCl_3$ was used as a solvent, unless otherwise noted. Chemical shifts (δ) are reported in ppm with respect to internal tetramethylsilane (δ = 0 ppm) or undeuterated residual solvent (i.e., $CHCl_3$ (δ = 7.265 ppm)). Coupling constants are given in hertz. Coupling patterns are indicated as follows: m = multiplet, d = doublet, s = singlet, br = broad. High-resolution mass spectrometry (HRMS) was conducted in the electron spray ionization (ESI)-time-of-flight

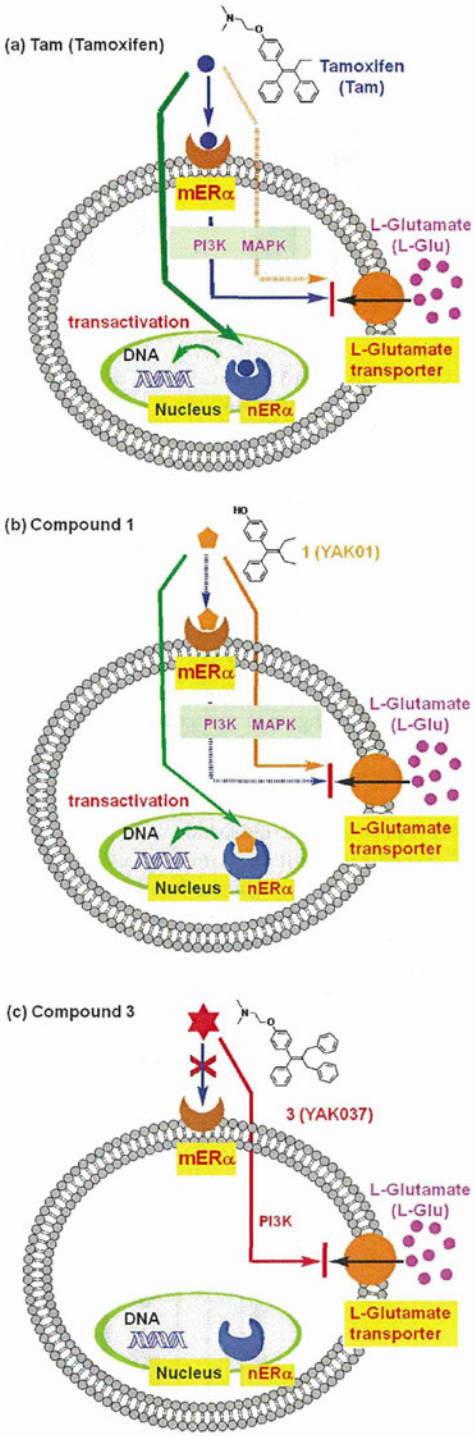

Figure 8. Schematic illustration of the proposed mechanisms of the effects of tamoxifen (a) and compounds **1** (b) and **3** (c).

(TOF) detection mode on a Bruker micrOTOF-05. FAB-MS and high-resolution FAB-MS were obtained on a JMS700-MSTATION (JEOL, Japan). Column chromatography was carried out on silica gel (silica gel 60N (100−210 μm), Kanto Chemicals, Japan). Flash column chromatography was performed on silica gel H (Merck, Germany). Analytical thin-layer chromatography (TLC) was performed on

precoated plates of silica gel HF_{254} (Merck, Germany). All the melting points were measured with a Yanaco Micro Melting Point apparatus and are uncorrected. Combustion analyses were carried out in the microanalysis laboratory of this faculty.

Synthesis of Compounds. Compounds **1** and **2** were synthesized from 4-hydroxybenzophenone and butyl-3-one or dibenzylacetone by using $TiCl_4$ in the presence of Zn. Introduction of the *N,N*-dimethylaminoethyl moiety at the phenolic hydroxyl group of **1** and **2** was carried out by base treatment, followed by addition of 2-dimethylaminoethyl chloride hydrochloride.

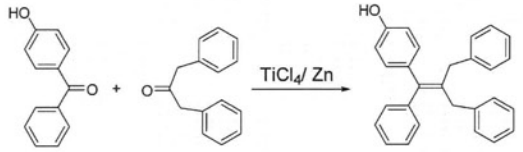

2 (YAK050)

Synthesis of Tamoxifen-Related Compounds. Compound 2 (YAK050). To a suspension of Zn powder (916.6 mg; 6.9 equiv with respect to 4-hydroxybenzophenone) in dry THF (30 mL) in a 200 mL three-necked flask, $TiCl_4$ (0.61 mL, 2.8 equiv) was added dropwise under an argon atmosphere at −20 °C (in an ice-salt bath) over 2 min. The resulting light green-yellow mixture was stirred at −20 °C for 20 min and then the cooling bath was removed. After 20 min, the flask was immersed in a preheated oil bath at 100 °C and refluxed at 100 °C with stirring for 2.5 h. To the resulting deep blue mixture was added in one portion a solution of 4-hydroxybenzophenone (401.3 mg, 2.02 mmol) and dibenzyl ketone (1.2735 g, 3 equiv) in 50 mL of dry THF. The resultant mixture was heated at reflux at 100 °C with stirring for 2 h, then allowed to cool to rt, and poured into 400 mL of 0.5 N aqueous NaOH solution. The whole was extracted with ethyl acetate (500 mL). The organic layer was washed with water, dried over $MgSO_4$ and evaporated to give a pale yellow oil (1.5172 g), which was column-chromatographed (silica gel, acetone/*n*-hexane (1:7)) to give 365.0 mg (48% yield) of the olefin **2** as a white amorphous solid. Mp: 57−60 °C. ^{1}H NMR ($CDCl_3$): δ: 7.287−7.079 (m, 17H), 6.760 (d, 2H, J = 8.8 Hz), 4.792 (s, 1H), 3.413 (s, 2H), 3.377 (s, 2H). ^{13}C NMR ($CDCl_3$): δ: 154.1, 143.0, 140.7, 140.4, 135.8, 135.4, 130.7, 129.4, 128.8, 128.3, 128.3, 128.2, 126.5, 125.9, 115.1, 37.4, 37.2. HRMS (ESI^-): Calcd. for $C_{28}H_{23}O$ ($[M - H]^-$), 375.1754. Found: 375.1744. Anal. Calcd for $C_{28}H_{24}O{\cdot}0.2H_2O$: C, 88.48; H, 6.47; N, 0.00. Found: C, 88.36; H, 6.63; N, 0.00.

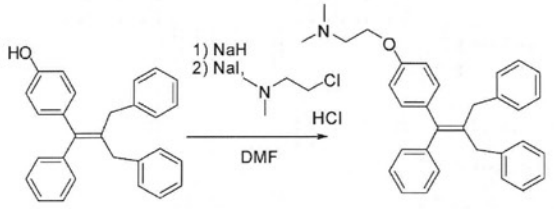

2 (YAK050)

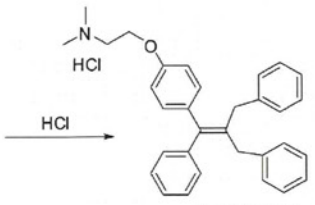

3 (YAK037)

Compound 3 (YAK037). To a suspension of NaH (60%, 42 mg, 1.05 mmol) in DMF (3 mL) at 0 °C was added a solution of the phenol **2** (158.2 mg, 0.420 mmol) in DMF (3 mL). The reaction mixture was stirred for 30 min at 0 °C, and then a solution of 2-dimethylaminoethyl chloride hydrochloride (181.0 mg, 1.256 mmol, 3.0 equiv) and NaI (94.0 mg, 0.627 mmol, 1.5 equiv) in DMF (3 mL) was added. The reaction mixture was stirred at 50 °C for 30 min, and then saturated aqueous NH_4Cl was added to quench the reaction. The mixture was extracted with Et_2O. The organic layer was washed with brine, dried over Na_2SO_4 and evaporated to afford a residue, which was column-chromatographed (ethyl acetate/Et_3N = 100/1) to give the intermediate amine (83.0 mg, 44% yield). The HCl salt of the resultant amine was prepared by repeated addition of a solution of 2 N HCl in Et_2O to a solution of the amine in ethyl acetate, followed by evaporation of the organic solvent to give **3**.

3: White solid. Mp. 169−170 °C. ^{1}H NMR ($CDCl_3$): δ: 13.073 (brs, 1H), 7.306−7.195 (m, 13H), 7.102−7.074 (m, 4H), 6.832 (d, 2H, J = 8.8 Hz), 4.481−4.459 (m, 2H), 3.425−3.390 (m, 6H), 2.893 (s, 6H). ^{13}C NMR ($CDCl_3$) δ: 155.7, 142.8, 140.4, 140.3, 140.2, 136.8, 136.2, 130.9, 129.4, 128.8, 128.7, 128.4, 128.3, 128.3, 126.6, 126.0, 125.9, 114.3, 62.8, 56.5, 43.6, 37.4, 37.2. HRMS (ESI^+, $[M + H]^+$): Calcd. for $C_{32}H_{34}NO$, 448.26349. Found: 448.26092. Anal. Calcd for $C_{32}H_{34}ClNO{\cdot}1/4H_2O$: C, 78.67; H, 7.12; N, 2.87. Found: C, 78.64; H, 7.30; N, 2.87.

Compound 1 (YAK01).

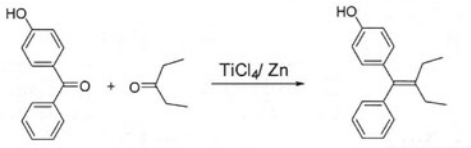

1 (YAK01)

To a suspension of Zn (0.86 g, 13.2 mmol) in 30 mL of dry THF at −5 °C was added dropwise $TiCl_4$ (0.72 mL, 6.6 mmol) under an argon atmosphere. The mixture was heated at reflux for 2 h. A solution of 4-hydroxybenzophenone (341.1 mg, 1.7 mmol) and 3-pentanone (0.50 mL, 5.0 mmol) in 50 mL of dry THF was added in one portion, and heating was continued at reflux for 6 h. Then the reaction mixture was cooled to rt, quenched with 10% aqueous K_2CO_3 (100 mL) and extracted with ethyl acetate (3 × 80 mL). The combined organic phase was washed with brine (50 mL), dried over Na_2SO_4, and evaporated to give a residue, which was flash column-chromatographed (3:1 hexane/ethyl acetate) to afford **1** (383.4 mg, 88.3%) as a white solid.

1: Mp. 76.0−76.5 °C (colorless needles, recrystallized from *n*-hexane). ^{1}H NMR ($CDCl_3$) δ: 7.261 (2H, t, J = 8.0 Hz), 7.173 (1H, d, J = 7.2 Hz), 7.128 (2H, d, J = 7.6 Hz), 7.009 (2H, d, J = 8.8 Hz), 6.726 (2H, d, J = 8.8 Hz), 4.763 (1H, s), 2.152 (2H, quartet, J = 7.6 Hz), 2.115 (2H, quartet, J = 6.0 Hz), 1.007 (3H, t, J = 7.6 Hz), 0.994 (3H, t, J = 7.6 Hz). ^{13}C NMR ($CDCl_3$) δ: 153.7, 143.7, 142.0, 136.5, 136.2, 130.5, 129.2, 127.9, 125.9, 114.8, 24.4, 24.3, 13.3. HRMS (ESI^-, $[M - H]^-$): Calcd. for $C_{18}H_{19}O^-$, 251.14414. Found: 251.14730. HRMS (FAB-MS, $[M]^+$) Calcd. for $C_{18}H_{20}O$, 252.1514. Found: 252.1528. Anal. Calcd. for $C_{18}H_{20}O$: C, 85.67; H, 7.99; N, 0.00. Found: C, 85.38; H, 8.13; N, 0.00.

Compound 4 (YAK06).

2-Dimethylaminoethyl chloride hydrochloride (282.4 mg, 2.0 mmol) and K_2CO_3 (1.5734 g, 11.4 mmol) were stirred in acetone/H_2O (18 mL/2 mL) at 0 °C for 30 min, then compound **1** (139.1 mg, 0.55 mmol) and K_2CO_3 (421.1 mg, 3.1 mmol) were added, and the whole was heated at reflux for 24 h, then cooled to rt. Inorganic materials were removed by filtration, and the filtrate was evaporated. The residue was flash column-chromatographed (100:1 ethyl acetate/Et_3N) to afford the amine as a white solid (88.0 mg). To a solution of the amine in ethyl acetate, a solution of HCl in ether was added to give a precipitate, which was collected and recrystallized from ethanol/ethyl acetate to give **4** (95.0 mg, 48%) as a white powder. **4**: Mp. 129.5−130.2 °C. ^{1}H NMR ($CDCl_3$) δ 726−6.90 (9H, m), 4.07 (2H, t, J = 6.0 Hz), 2.75 (2H, t, J = 6.0 Hz), 2.40 (6H, s), 2.15 (4H, d, J = 7.2 Hz), 1.00 (6H, t, J = 7.2 Hz). HRMS (FAB-MS, $[M\text{-}Cl]^+$): Calcd. for $C_{22}H_{30}NO^+$: 324.2322. Found: 324.2321.

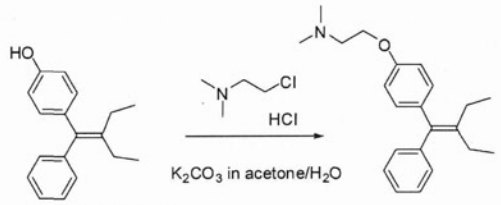

1 (YAK01)

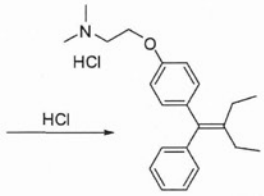

4 (YAK06)

Biology. All procedures using live animals in this study were conducted in accordance with the guidelines of the National Institute of Health Sciences, Japan.

Materials. Dulbecco's modified Eagle's medium (DMEM) and fetal bovine serum (FBS) were purchased from GIBCO (CA, USA). Glutamate dehydrogenase (GLD) was purchased from Roche (Mannheim, Germany). β-Nicotinamide adenine dinucleotide (βNAD), 3-(4,5-dimethyl-2-thiazolyl)-2,5-diphenyl-2H-tetrazolium bromide (MTT), 1-methoxy-5-methylphenazinium methyl sulfate (MPMS), lactate lithium salt and LY294002 were purchased from Sigma (MO, USA). DL-threo-β-benzyloxyaspartic acid (TBOA) and ICI182,780 were purchased from Tocris (MO, USA). U0126 was purchased from Promega (WI, USA). Assay kits for hormonal effects on HEK293/hERα and HEK293/hERβ reporter cells were purchased from Clontech (CA, USA).

Cell Culture. Primary cultures of astrocytes were prepared from the cerebral cortices of 3-day-old neonates of Wistar rats, as described previously.[31] Briefly, dissociated cortical cells were suspended in modified DMEM containing 30 mM glucose, 2 mM glutamine, 1 mM pyruvate and 10% FBS, and plated on uncoated 75 cm^2 flasks at the density of 600 000 cells/cm^2. A monolayer of type I astrocytes was obtained 12−14 days after plating. Nonastrocytes such as microglia were detached from the flasks by shaking and removed by changing the medium. Astrocytes in the flasks were dissociated by trypsinization, reseeded on uncoated 96-well microtiter plates at 20 000 cells/cm^2, and incubated until the cells became confluent (approximately 9−10 days after reseeding). In this culture, >98% of the cells were identified as type I astrocytes on the basis of positivity for GFAP and flattened, polygonal appearance.

Measurement of Extracellular L-Glu Concentration. Extracellular L-Glu concentration was measured by means of a colorimetric method according to Abe et al.[32] Briefly, 50 μL of culture supernatant was transferred to each well of a 96-well microtiter plate and mixed with 50 μL of substrate mixture consisting of 20 U/mL GLD, 2.5 mg/mL β-NAD, 0.25 mg/mL MTT, 100 μM MPMS and 0.1% (v/v) Triton X-100 in 0.2 M Tris-HCl buffer (pH 8.2). After 10 min incubation at 37 °C, the reaction was stopped by adding 100 μL of solution containing 50% (v/v) dimethylformamide and 20% (wt/vol) SDS (pH 4.7). In this reaction, MTT (yellow) is converted into MTT formazan (purple) in proportion to the L-Glu concentration. The amount of MTT formazan was determined by measuring the absorbance at 570 nm (test wavelength) and 655 nm (reference wavelength) with a microplate reader. The concentration of L-Glu was estimated from a standard curve, which was constructed in each assay using cell-free medium containing known concentrations of L-Glu. L-Glu clearance was shown as the amount of L-Glu taken up by astrocytes, which was calculated from the concentration difference in the medium.

Treatment with Test Compounds. L-Glu was dissolved at 1 mM in phosphate-buffered saline and diluted to 100 μM with the culture medium. Compounds **1**, **2**, **3**, and **4** were dissolved at 100, 100, 100, and 10 mM, respectively, in dimethyl sulfoxide (DMSO) and diluted to the required final concentrations with the culture medium. The concentration of DMSO in the medium was controlled to be below 0.1%, because we had already confirmed that 0.1% DMSO has no effect on L-Glu transport activity or cell viability (data not shown). Cells were incubated with test compounds for 24 h. TBOA (IC50 = 48 μM for GLAST, 7 μM for GLT1) was freshly dissolved at 1 mM in culture medium for each experiment. ICI182,780 (IC50 = 0.29 nM for ERs), U0126 (IC50 = 72 nM for MEK1, 58 nM for MEK2), and LY294002 (IC50 = 1 μM for class 1 PI3K, 19 μM for class 2 PI3K) were dissolved at 1, 5, and 5 mM, respectively, in DMSO, and the solutions were diluted with culture medium to yield the required final concentrations. These inhibitors were coapplied with 1 nM test compounds (**1**−**4**) for 24 h.

Assay Procedure for Hormonal Effects on HEK293/hERα and HEK293/hERβ Reporter Cells. Human embryo kidney 293 cells (HEK293) were grown in FBS (+) DMEM in 100 mm dishes. Cells were subcultured once or twice a week at about 80% confluence. A solution of 12.4 μL of 2 M calcium ion, 100 ng/well reporter or negative control vector (pERE-TA-SEAP or pTA-SEAP, Clontech), 50 ng/well expression vector (pcDNA3 ERα or pcDNA3 ERβ, generous gift from Dr. Shige-aki Kato, University of Tokyo, Japan), and 100 ng/well positive control vector (pSV-β-galactosidase, Promega) was diluted to a final volume of 10 μL/well. This mixture was carefully added dropwise to the same volume of HEPES solution with slow vortexing, and the mixture was incubated at rt for 20 min to obtain a precipitate. Cells from the exponential growth phase were seeded (3.0×10^4 cells/ml) into 96-well plates the day before transfection. The cells were incubated with fresh medium for 1 h, then 1/10 volume of precipitate was added to each well and incubation was continued for 24 h at 37 °C in an atmosphere of 5% CO_2 in air. The medium was replaced with fresh FBS (-) medium and incubation was continued for a further 24 h. Then the cells were incubated with test compounds for 24 h at 37 °C in an atmosphere of 5% CO_2 in air. SEAP activity (Great EscapeTM SEAP chemiluminescence kit 2.0, Clontech) and β-galactosidase activity (β-Galactosidase Enzyme Assay System with Reporter Lysis Buffer, Promega) were measured with a Spectramax M5 microplate reader (Molecular Devices Japan, Tokyo, Japan). All transfections were performed in triplicate.

Statistical Analysis. Data were obtained from four independent experiments (averaged values of six wells for each) unless otherwise noted. Data are expressed as means ± SEM of these data. Tests of homogeneity of variance, normality, and distribution were performed to ensure that the assumptions required for standard parametric ANOVA were satisfied. Statistical analysis was performed by one-way repeated-measures ANOVA with post hoc Tukey's test for multiple pairwise comparisons.

■ AUTHOR INFORMATION

Corresponding Author

*(K.S.) Telephone and Fax: +81-3-3700-9698. E-mail: kasato@nihs.go.jp. (T.O.) Telephone: +81-3-5840-4730. Fax: +81-3-5840-4735. E-mail: ohwada@mol.f.u-tokyo.ac.jp.

Author Contributions

†These two authors equally contributed to this Article. Individual author contributions: K.S. designed the biological experimental plan, performed biological experiments, data analysis, manuscript writing and preparation. J.K. and Y.S. performed experimental work. K.T. contributed to the data analysis. J.O., K.N. and Y.S. provided advice on the experimental direction. Y.O. carried out organic synthesis, data analysis and wrote portions of the manuscript. Y.S. carried out organic synthesis. T.O. designed and oversaw all organic chemistry studies, carried out organic synthesis and also performed data analysis and manuscript writing and preparation.

Funding

This work was partly supported by a Grant-in-Aid from the Food Safety Commission, Japan (No. 1003), a Grant-in-Aid for Young Scientists from MEXT, Japan (KAKENHI 21700422), the Program for Promotion of Fundamental Studies in Health Sciences of NIBIO, Japan, a Health and Labor Science Research Grant for Research on Risks of Chemicals, a Health and Labor Science Research Grant for Research on New Drug Development from MHLW, Japan, awarded to K.S., and a Health and Labor Science Research Grant for Research on Risks of Chemicals from MHLW, Japan, awarded to K.N. and T.O.

Notes

The authors declare no competing financial interest.

■ ACKNOWLEDGMENTS

We thank Dr. Shige-aki Kato for providing pcDNA3 hERα and pcDNA3 hERβ.

■ ABBREVIATIONS

βNAD; β-nicotinamide adenine dinucleotide; CNS; central nervous system; DMEM; Dulbecco's modified Eagle's medium; DMSO; dimethyl sulfoxide; E2; 17β-estradiol; ESI; electron spray ionization; FBS; fetal bovine serum; GLD; glutamate dehydrogenase; HEK-293; Human embryo kidney 293 cells; HRMS; high-resolution mass spectrometry; L-Glu; L-glutamate; MAPK; mitogen-activated protein kinase; MEK; mitogen-activated protein kinase/extracellular signal-regulated kinase; mERα; membrane-associated estrogen receptor α; mGluR5; metabotropic glutamate receptor 5; MPMS; 1-methoxy-5-methylphenazinium methyl sulfate; MTT; 3-(4,5-dimethyl-2-thiazolyl)-2,5-diphenyl-2H-tetrazolium bromide; nERs; nuclear estrogen receptors; PI3K; phosphatidylinositol 3-kinase; Tam; tamoxifen; TBOA; DL-threo-β-benzyloxyaspartic acid; TLC; thin-layer chromatography; TOF; time-of-flight

■ REFERENCES

(1) Kumar, A., Singh, R. L., and Babu, G. N. (2010) Cell death mechanisms in the early stages of acute glutamate neurotoxicity. *Neurosci. Res. 66*, 271–278.

(2) Choi, D. W. (1988) Glutamate neurotoxicity and diseases of the nervous system. *Neuron 1*, 623–634.

(3) Logan, W. J., and Snyder, S. H. (1971) Unique high affinity uptake systems for glycine, glutamic and aspartic acids in central nervous tissue of the rat. *Nature 234*, 297–299.

(4) Beart, P. M., and O'Shea, R. D. (2007) Transporters for L-glutamate: an update on their molecular pharmacology and pathological involvement. *Br. J. Pharmacol. 150*, 5–17.

(5) Sato, K., Matsuki, N., Ohno, Y., and Nakazawa, K. (2003) Estrogens inhibit L-glutamate uptake activity of astrocytes via membrane estrogen receptor alpha. *J. Neurochem. 86*, 1498–1505.

(6) Olivier, S., Close, P., Castermans, E., de Leval, L., Tabruyn, S., Chariot, A., Malaise, M., Merville, M. P., Bours, V., and Franchimont, N. (2006) Raloxifene-induced myeloma cell apoptosis: a study of nuclear factor-kappaB inhibition and gene expression signature. *Mol. Pharmacol. 69*, 1615–1623.

(7) Sato, K., Saito, Y., Oka, J., Ohwada, T., and Nakazawa, K. (2008) Effects of tamoxifen on L-glutamate transporters of astrocytes. *J. Pharmacol. Sci. 107*, 226–230.

(8) Bunch, L., Erichsen, M. N., and Jensen, A. A. (2009) Excitatory amino acid transporters as potential drug targets. *Expert Opin. Ther. Targets 13*, 719–731.

(9) Margueron, R., Duong, V., Bonnet, S., Escande, A., Vignon, F., Balaguer, P., and Cavailles, V. (2004) Histone deacetylase inhibition and estrogen receptor alpha levels modulate the transcriptional activity of partial antiestrogens. *J. Mol. Endocrinol. 32*, 583–594.

(10) Thompson, D. S., Spanier, C. A., and Vogel, V. G. (1999) The relationship between tamoxifen, estrogen, and depressive symptoms. *Breast J. 5*, 375–382.

(11) Grilli, S. (2006) Tamoxifen (TAM): the dispute goes on. *Ann. Ist. Super. Sanita 42*, 170–173.

(12) Sha, Y., Tashima, T., Mochizuki, Y., Toriumi, Y., Adachi-Akahane, S., Nonomura, T., Cheng, M., and Ohwada, T. (2005) Compounds structurally related to tamoxifen as openers of large-conductance calcium-activated K^+ channel. *Chem. Pharm. Bull. (Tokyo) 53*, 1372–1373.

(13) Robertson, D. W., Katzenellenbogen, J. A., Long, D. J., Rorke, E. A., and Katzenellenbogen, B. S. (1982) Tamoxifen antiestrogens. A comparison of the activity, pharmacokinetics, and metabolic activation of the cis and trans isomers of tamoxifen. *J. Steroid Biochem. 16*, 1–13.

(14) Weltje, L., vom Saal, F. S., and Oehlmann, J. (2005) Reproductive stimulation by low doses of xenoestrogens contrasts with the view of hormesis as an adaptive response. *Hum. Exp. Toxicol. 24* (9), 431–437.

(15) Perego, C., Vanoni, C., Bossi, M., Massari, S., Basudev, H., Longhi, R., and Pietrini, G. (2000) The GLT-1 and GLAST glutamate transporters are expressed on morphologically distinct astrocytes and regulated by neuronal activity in primary hippocampal co-cultures. *J. Neurochem. 75*, 1076–1084.

(16) Guillet, B., Lortet, S., Masmejean, F., Samuel, D., Nieoullon, A., and Pisano, P. (2002) Developmental expression and activity of high affinity glutamate transporters in rat cortical primary cultures. *Neurochem. Int. 40*, 661–671.

(17) Razandi, M., Pedram, A., Greene, G. L., and Levin, E. R. (1999) Cell membrane and nuclear estrogen receptors (ERs) originate from a single transcript: studies of ERalpha and ERbeta expressed in Chinese hamster ovary cells. *Mol. Endocrinol. 13*, 307–319.

(18) Pappas, T. C., Gametchu, B., and Watson, C. S. (1995) Membrane estrogen receptors identified by multiple antibody labeling and impeded-ligand binding. *FASEB J. 9*, 404–410.

(19) Grove-Strawser, D., Boulware, M. I., and Mermelstein, P. G. (2010) Membrane estrogen receptors activate the metabotropic glutamate receptors mGluR5 and mGluR3 to bidirectionally regulate CREB phosphorylation in female rat striatal neurons. *Neuroscience 170*, 1045–1055.

(20) Mannella, P., and Brinton, R. D. (2006) Estrogen receptor protein interaction with phosphatidylinositol 3-kinase leads to activation of phosphorylated Akt and extracellular signal-regulated kinase 1/2 in the same population of cortical neurons: a unified mechanism of estrogen action. *J. Neurosci. 26*, 9439–9447.

(21) Szego, E. M., Barabas, K., Balog, J., Szilagyi, N., Korach, K. S., Juhasz, G., and Abraham, I. M. (2006) Estrogen induces estrogen receptor alpha-dependent cAMP response element-binding protein phosphorylation via mitogen activated protein kinase pathway in basal forebrain cholinergic neurons in vivo. *J. Neurosci. 26*, 4104–4110.

(22) Vasudevan, N., Kow, L. M., and Pfaff, D. (2005) Integration of steroid hormone initiated membrane action to genomic function in the brain. *Steroids 70*, 388–396.

(23) Alyea, R. A., Laurence, S. E., Kim, S. H., Katzenellenbogen, B. S., Katzenellenbogen, J. A., and Watson, C. S. (2008) The roles of membrane estrogen receptor subtypes in modulating dopamine transporters in PC-12 cells. *J. Neurochem. 106* (4), 1525–1533.

(24) Watson, C. S., Alyea, R. A., Hawkins, B. E., Thomas, M. L., Cunningham, K. A., and Jakubas, A. A. (2006) Estradiol effects on the dopamine transporter - protein levels, subcellular location, and function. *J. Mol. Signaling 1*, 5.

(25) Filardo, E. J., and Thomas, P. (2005) GPR30: a seven-transmembrane-spanning estrogen receptor that triggers EGF release. *Trends. Endocrinol. Metab. 16* (8), 362–367.

(26) Revankar, C. M., Cimino, D. F., Sklar, L. A., Arterburn, J. B., and Prossnitz, E. R. (2005) A transmembrane intracellular estrogen receptor mediates rapid cell signaling. *Science 11;307* (5715), 1625–1630.

(27) Filardo, E. J., Quinn, J. A., Bland, K. I., and Frackelton, A. R. Jr. (2000) Estrogen-induced activation of Erk-1 and Erk-2 requires the G

protein-coupled receptor homolog, GPR30, and occurs via transactivation of the epidermal growth factor receptor through release of HB-EGF. *Mol. Endocrinol. 14* (10), 1649−1660.

(28) Thomas, P., Pang, Y., Filardo, E. J., and Dong, J. (2005) Identity of an estrogen membrane receptor coupled to a G protein in human breast cancer cells. *Endocrinology 146* (2), 624−632.

(29) Kuo, J., Hamid, N., Bondar, G., Prossnitz, E. R., and Micevych, P. (2010) Membrane estrogen receptors stimulate intracellular calcium release and progesterone synthesis in hypothalamic astrocytes. *J. Neurosci. 30* (39), 12950−12957.

(30) Kisanga, E. R., Gjerde, J., Guerrieri-Gonzaga, A., Pigatto, F., Pesci-Feltri, A., Robertson, C., Serrano, D., Pelosi, G., Decensi, A., and Lien, E. A. (2004) Tamoxifen and metabolite concentrations in serum and breast cancer tissue during three dose regimens in a randomized preoperative trial. *Clin. Cancer Res. 10*, 2336−2343.

(31) Suzuki, K., Ikegaya, Y., Matsuura, S., Kanai, Y., Endou, H., and Matsuki, N. (2001) Transient upregulation of the glial L-glutamate transporter GLAST in response to fibroblast growth factor, insulin-like growth factor and epidermal growth factor in cultured astrocytes. *J. Cell Sci. 114*, 3717−3725.

(32) Abe, K., Abe, Y., and Saito, H. (2000) Evaluation of L-glutamate clearance capacity of cultured rat cortical astrocytes. *Biol. Pharm. Bull. 23*, 204−207.

Cell Mol Neurobiol
DOI 10.1007/s10571-012-9829-z

SHORT COMMUNICATION

Cell-Autonomous Enhancement of Glutamate-Uptake by Female Astrocytes

Yosuke Morizawa · Kaoru Sato · Junpei Takaki · Asami Kawasaki · Keisuke Shibata · Takeshi Suzuki · Shigeru Ohta · Schuichi Koizumi

Received: 27 February 2012 / Accepted: 8 March 2012

Abstract Since gonadal female hormones act on and protect neurons, it is well known that the female brain is less vulnerable to stroke or other brain insults than the male brain. Although glial functions have been shown to affect the vulnerability of the brain, little is known if such a sex difference exists in glia, much less the mechanism that might cause gender-dependent differences in glial functions. In this study, we show that in vitro astrocytes obtained from either female or male pups show a gonadal hormone-independent phenotype that could explain the gender-dependent vulnerability of the brain. Female spinal astrocytes cleared more glutamate by GLAST than male ones. In addition, motoneurons seeded on female spinal astrocytes were less vulnerable to glutamate than those seeded on male ones. It is suggested that female astrocytes uptake more glutamate and reveal a stronger neuroprotective effect against glutamate than male ones. It should be noted that such an effect was independent of gonadal female hormones, suggesting that astrocytes have cell-autonomous regulatory mechanisms by which they transform themselves into appropriate phenotypes.

Keywords Astrocytes · Sex difference · GLAST · Glutamate · Neurotoxicity

Y. Morizawa · K. Shibata · S. Koizumi (✉)
Department of Neuropharmacology, Graduate School of Medicine and Engineering, University of Yamanashi, Yamanashi, Japan
e-mail: skoizumi@yamanashi.ac.jp

Y. Morizawa · S. Ohta
Graduate School of Biomedical Sciences, Hiroshima University, Hiroshima, Japan

K. Sato · J. Takaki
Division of Pharmacology, National Institute of Health Sciences, Tokyo, Japan

J. Takaki · T. Suzuki
Division of Basic Biological Sciences, Keio University, Tokyo, Japan

A. Kawasaki
Center for Trans-Disciplinary Research, Niigata University, Niigata, Japan

Introduction

Astrocytes control synaptic transmission by releasing gliotransmitters such as ATP and glutamate or by uptaking excess neurotransmitters (Haydon 2001; Koizumi et al. 2003). As for the clearance of neurotransmitters, astrocytes express excitatory amino acid transporter 1 (EAAT1; GLAST) or EAAT2 (GLT-1), by which they control the extracellular glutamate concentrations and excitatory neurotransmission. Thus, the functions of these transporters are highly involved in glutamate-dependent excitotoxicity or various neuronal diseases.

It is well known clinically and experimentally that female brain is more resistant to various brain insults or neurodegenerative diseases than male brain, and such sex differences have been historically attributed to the protective effect of gonadal female hormones such as estrogen. Studies by Sato et al. (2003) and Pawlak et al. (2005) have already shown that, exogenously applied 17β-estradiol (E2), the most potent mammalian estrogen, affects the activity of glutamate uptake in astrocytes, which may in part explain the gender difference in brain vulnerability. However, sexual dimorphism generally persists well beyond menopause (Sacco et al. 1998), suggesting that sex differences in brain injury may not be entirely related to the

Published online: 27 March 2012

influence of gonadal female hormones. In this study, we demonstrate that female astrocytes in vitro are a high glutamate-uptake phenotype that removes more glutamate and protects motoneurons more against glutamate than male ones. We also demonstrate that such a difference in astrocytic function does not depend on gonadal female hormones but depends rather on a local cell-autonomous mechanism (s).

Materials and Methods

All of the animals used in this study were obtained, housed, cared for, and used in accordance with the guidelines of the Universities of Yamanashi and Hiroshima.

Cell Culture

The culture of spinal astrocytes was prepared as described previously (Shibata et al. 2011) with minor modifications. The spinal cord was removed from neonatal male or female Wistar rats. Male and female rat pups were distinguished by the larger genital papilla and longer ano-genital distance in male versus female pups. To remove serum-derived hormones, charcoal-stripped fetal bovine serum was used. The culture of rat motoneurons was prepared as described previously (Nishijima et al. 2001).

Measurement of Glutamate Uptake

Glutamate clearance was measured as previously described (Sato et al. 2003).

Ca^{2+} Imaging in Single Motor Neurons

Changes in the intracellular Ca^{2+} concentration ($[Ca^{2+}]i$) were measured by the fura-2 method as previously described (Koizumi et al. 2003). The amplitude of the high K^+-evoked $[Ca^{2+}]i$ elevation in motoneurons seeded on either male or female astrocytes was used as an index of neuronal function (Koizumi et al. 1994).

Chemicals

DL-*threo*-β-Benzyloxyaspartic acid (TBOA) and Dihydrokainate (DHK) were purchased from TOCRIS Bioscience (Bristol, UK). Anti-neurofilament H non-phosphorylated (SMI-32) antibody was from COVANCE Japan Co. Ltd (Tokyo, Japan). All other reagents were from Sigma-Aldrich Japan (Tokyo, Japan).

Statistical Analysis

Experimental results are expressed as means ± S.E.M. Statistical analysis was performed using Student's *t* test. One way analyses of variance (ANOVA) followed by Tukey test were applied for multiple comparisons. The differences between means were considered to be significant when the *p* values were less than 5 %.

Results

Female astrocytes (grey columns) cleared significantly larger amounts of glutamate than male ones (open columns) both at 30 and 60 min (Fig. 1). At 30 min, female astrocytes showed two times higher glutamate uptake activity. When extracellular Na^+ was removed, the glutamate clearance disappeared almost completely (data not shown), indicating that the extracellular glutamate was uptaken by Na^+-dependent glutamate transporter(s). To identify the predominant glutamate transporter(s) of cultured astrocytes, we co-applied 0.3 mM TBOA, an inhibitor of both GLAST and GLT-1 (Shimamoto et al. 2004) or 1 mM DHK, a selective inhibitor of GLT-1 (Johnston et al. 1974) with glutamate. TBOA dramatically inhibited the glutamate uptake in both male and female astrocytes, whereas DHK showed only slight inhibition or no effect, suggesting that GLAST was dominant in both cultures.

We then investigated whether such sex-dependent differences in glutamate uptake might affect neuronal damage/death induced by exogenously applied glutamate. Since the glutamate clearance by spinal astrocytes greatly affects the survival of motoneurons (Jimonet et al. 1999),

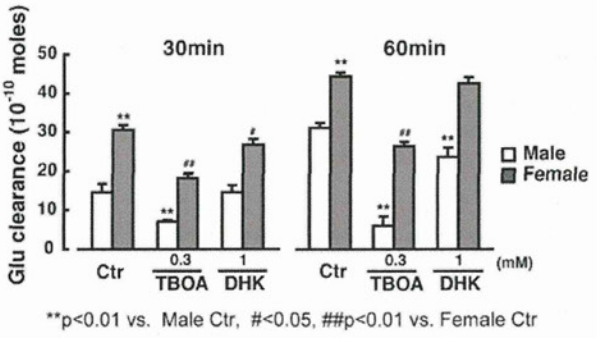

Fig. 1 Differences in glutamate (Glu) clearance in female and male astrocytes. The uptake activity of female (*grey columns*) and male (*open columns*) astrocytes, 30 and 60 min after incubation with glutamate in the absence (Ctr) and the presence (TBOA or DHK) of inhibitors of glutamate transporters. Female astrocytes uptook higher amounts of glutamate than male ones at both time periods (Ctr). DHK had no or only a slight effect on the glutamate uptake, but TBOA significantly decreased the glutamate clearance both in male and female astrocytes

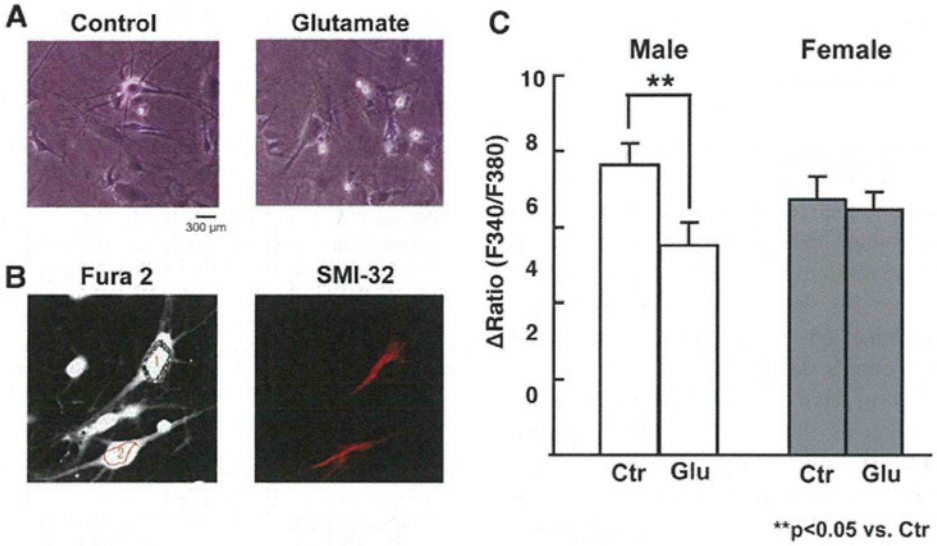

Fig. 2 Potent protection of motoneurons by female astrocytes. **a** Phase-contrast images of motoneurons seeded on male astrocytes, showing the effects of glutamate-treatment. *Left panel*, healthy motoneurons show phase bright morphology; *right panel*, motoneurons damaged by glutamate seeded on male astrocytes, show dark, flattened shape. **b** Fura-2 fluorescent images and immunostaining by SMI-32 antibody. *Left panel*, fura-2 fluorescence; *right panel*, immunocytochemical images of anti-SMI32 antibody of the motoneurons after Ca^{2+} imaging experiments. **c** The high K^+-evoked increase in $[Ca^{2+}]i$ in motoneurons after treatment of cells with glutamate (100 μM, 30 min, and then 24 h washout). Changes in $[Ca^{2+}]i$ in cells were expressed as Δ ratio of F340/F380. The high K^+-evoked increase in $[Ca^{2+}]i$ in motoneurons seeded on male astrocytes was decreased by glutamate but not in those seeded on female astrocytes

we used motoneurons cultured on either male or female spinal astrocytes. Figure 2a shows phase-contrast images of motoneurons, showing the effects of glutamate-treatment. Healthy motoneurons show phase bright morphology (left panel), but when damaged, they show a dark, flattened shape. Motoneurons were stimulated with glutamate (100 μM) for 30 min, and then washed-out and further incubated with glutamate-free medium for 24 h. The fraction of motoneurons with phase bright morphology was dramatically decreased by the glutamate-treatment. For quantitative analysis, we employed a high K^+-evoked increase in $[Ca^{2+}]i$ in neurons (Koizumi et al. 1994). The treatment with glutamate (100 μM, 30 min, and then 24 h washout) significantly decreased the high K^+-evoked responses in motoneurons on male astrocytes, whereas it had almost no effect on the $[Ca^{2+}]i$ responses in motoneurons on female astrocytes (Fig. 2c). After the Ca^{2+} imaging experiments, cells were stained with anti-SMI-32 antibody to confirm that the cells of interest were motoneurons (Fig. 2b, right).

Discussion

In this study, we demonstrated that (1) female astrocytes cleared more glutamate by GLAST than male ones; (2) spinal female astrocytes showed stronger protective action against glutamate-evoked neuronal damage in motoneurons than male ones; and most importantly, (3) these characteristic features of female astrocytes were not necessarily dependent on gonadal female hormones, since astrocytes were obtained separately from either female or male pups and cultured in the absence of sex hormones. Although differences in the vulnerability to several types of brain insults between female and male brains are often explained by the fact that gonadal female hormones act on and protect neurons, it is unlikely that such differences are entirely related to the hormonal effects on neurons. Thus, our present results could be novel and important as that we have shown that such sex differences could be explained by (i) functional differences in astrocytes but not neurons, and that (ii) these differences in astrocytic functions do not totally depend on gonadal sex hormones but, presumably, depend on the property of XX versus XY chromosomes, by which each astrocyte is transformed into a distinct phenotype in a cell-autonomous mechanism, although we must await further studies to clarify the detail molecular mechanisms.

As for the peripheral sex hormone-independent mechanisms, extragonadal production of E2 may be involved. E2 can be synthesized locally from testosterone by the aromatase cytochrome P450 in the CNS. In an experimental stroke model, mice with targeted deletion of *cyp*19, which codes for aromatase P450, showed more severe brain injury

than wild-type litter mates (McCullough et al. 2003), suggesting that aromatase and extragonadal E2 play an important role in protection of the brain. It should be noted that astrocytes express aromatase P450, and more importantly, that the expression of P450 is higher in female astrocytes than that in male astrocytes (Liu et al. 2007). These findings suggest that female astrocytes locally produce more estrogen than male, thereby leading to higher expression of glutamate-transporters. The higher capacity to clear glutamate causes the female astrocytes to have higher neuroprotection against glutamate. However, further study is required to clarify this issue.

Spinal astrocytes in vivo express more GLT-1 than GLAST. It is well known that, similar to cultured astrocytes obtained from the hippocampus or cortex, GLT-1 expression becomes less dominant by cultivation. If cultured with neurons, or in the presence of several factors such as cAMP-forming reagents or β-lactam antibiotics, GLT-1 expression is increased (Rothstein et al. 2005). When spinal astrocytes were co-cultured with motoneurons, it is possible that GLT-1 was upregulated contributing to the clearance of glutamate in female astrocytes. Thus, we do not exclude the involvement of GLT-1 in the higher uptake of glutamate in female astrocytes.

Taken together, we demonstrated that spinal astrocytes obtained from female pups showed higher glutamate uptake activity and more intensive neuroprotection against glutamate than those obtained from males. The effect was independent of gonadal female hormones, suggesting that astrocytes have cell-autonomous regulatory mechanisms by which they transform themselves into less vulnerable phenotypes.

Acknowledgments This study was partly supported by a Grand-in Aid for Scientific Research [(to SK)(A) 21240034], Grants-in-Aid for challenging Exploratory Research [(to SK) 23659810], by a Grant-in-Aid [(to SK and KS) 1003] from Food Safety Commission Japan, and by Diichi-Sankyo Foundation of Life Science.

References

Haydon PG (2001) GLIA: listening and talking to the synapse. Nat Rev Neurosci 2:185–193

Jimonet P, Audiau F, Barreau M, Blanchard JC, Boireau A, Bour Y, Coleno MA, Doble A, Doerflinger G, Huu CD, Donat MH, Duchesne JM, Ganil P, Gueremy C, Honor E, Just B, Kerphirique R, Gontier S, Hubert P, Laduron PM, Le Blevec J, Meunier M, Miquet JM, Nemecek C, Mignani S et al (1999) Riluzole series. Synthesis and in vivo "antiglutamate" activity of 6-substituted-2-benzothiazolamines and 3-substituted-2-imino-benzothiazolines. J Med Chem 42:2828–2843

Johnston GA, Curtis DR, Davies J, McCulloch RM (1974) Spinal interneurone excitation by conformationally restricted analogues of L-glutamic acid. Nature 248:804–805

Koizumi S, Kataoka Y, Niwa M, Yamashita K, Taniyama K, Kudo Y (1994) Endothelin increased [$Ca2^{+}$]i in cultured neurones and slices of rat hippocampus. Neuroreport 5:1077–1080

Koizumi S, Fujishita K, Tsuda M, Shigemoto-Mogami Y, Inoue K (2003) Dynamic inhibition of excitatory synaptic transmission by astrocyte-derived ATP in hippocampal cultures. Proc Natl Acad Sci USA 100:11023–11028

Liu M, Hurn PD, Roselli CE, Alkayed NJ (2007) Role of P450 aromatase in sex-specific astrocytic cell death. J Cereb Blood Flow Metab 27:135–141

McCullough LD, Blizzard K, Simpson ER, Oz OK, Hurn PD (2003) Aromatase cytochrome P450 and extragonadal estrogen play a role in ischemic neuroprotection. J Neurosci 23:8701–8705

Nishijima C, Kimoto K, Arakawa Y (2001) Survival activity of troglitazone in rat motoneurones. J Neurochem 76:383–390

Pawlak J, Brito V, Kuppers E, Beyer C (2005) Regulation of glutamate transporter GLAST and GLT-1 expression in astrocytes by estrogen. Brain Res Mol Brain Res 138:1–7

Rothstein JD, Patel S, Regan MR, Haenggeli C, Huang YH, Bergles DE, Jin L, Dykes Hoberg M, Vidensky S, Chung DS, Toan SV, Bruijn LI, Su ZZ, Gupta P, Fisher PB (2005) Beta-lactam antibiotics offer neuroprotection by increasing glutamate transporter expression. Nature 433:73–77

Sacco RL, Boden-Albala B, Gan R, Chen X, Kargman DE, Shea S, Paik MC, Hauser WA (1998) Stroke incidence among white, black, and hispanic residents of an urban community: the northern manhattan stroke study. Am J Epidemiol 147:259–268

Sato K, Matsuki N, Ohno Y, Nakazawa K (2003) Estrogens inhibit l-glutamate uptake activity of astrocytes via membrane estrogen receptor alpha. J Neurochem 86:1498–1505

Shibata K, Sugawara T, Fujishita K, Shinozaki Y, Matsukawa T, Suzuki T, Koizumi S (2011) The astrocyte-targeted therapy by Bushi for the neuropathic pain in mice. PLoS ONE 6:e23510

Shimamoto K, Sakai R, Takaoka K, Yumoto N, Nakajima T, Amara SG, Shigeri Y (2004) Characterization of novel L-threo-beta-benzyloxyaspartate derivatives, potent blockers of the glutamate transporters. Mol Pharmacol 65:1008–1015

Metallomics

RSC Publishing

PAPER

AMP-activated protein kinase-mediated glucose transport as a novel target of tributyltin in human embryonic carcinoma cells†

Cite this: DOI: 10.1039/c3mt20268b

Shigeru Yamada,[a] Yaichiro Kotake,[b] Yuko Sekino[a] and Yasunari Kanda*[a]

Organotin compounds such as tributyltin (TBT) are known to cause various forms of cytotoxicity, including developmental toxicity and neurotoxicity. However, the molecular target of the toxicity induced by nanomolar levels of TBT has not been identified. In the present study, we found that exposure to 100 nM TBT induced growth arrest in human pluripotent embryonic carcinoma cell line NT2/D1. Since glucose provides metabolic energy, we focused on the glycolytic system. We found that exposure to TBT reduced the levels of both glucose-6-phosphate and fructose-6-phosphate. To investigate the effect of TBT exposure on glycolysis, we examined glucose transporter (GLUT) activity. TBT exposure inhibited glucose uptake *via* a decrease in the level of cell surface-bound GLUT1. Furthermore, we examined the effect of AMP-activated protein kinase (AMPK), which is known to regulate glucose transport by facilitating GLUT translocation. Treatment with the potent AMPK activator, AICAR, restored the TBT-induced reduction in cell surface-bound GLUT1 and glucose uptake. In conclusion, these results suggest that exposure to nanomolar levels of TBT causes growth arrest by targeting glycolytic systems in human embryonic carcinoma cells. Thus, understanding the energy metabolism may provide new insights into the mechanisms of metal-induced cytotoxicity.

Received 28th December 2012,
Accepted 20th February 2013

DOI: 10.1039/c3mt20268b

www.rsc.org/metallomics

Introduction

Growing evidence suggests that environmental metals contribute to developmental toxicity and neurotoxicity.[1–3] Since the developing brain is inherently more vulnerable to injury than the adult brain, exposure to metals during early fetal development can potentially cause neurological disorders at doses much lower than those that are toxic in adults.[4–7] Therefore, it is necessary to elucidate the cytotoxic effects of such metals at low levels.

Organotin compounds are well known to cause cytotoxicity. Although organotin compounds or derivatives have been shown to have a potential anti-tumor activity[8,9] and some of them have already been entered into preclinical trials,[10] tributyltin (TBT) is considered to be associated with developmental toxicity and neurotoxicity.[11] For example, TBT can cause increased fetal mortality, decreased fetal birth weights, and behavioral abnormalities in rat offspring.[12,13] TBT is known to affect fertilization and embryonic development.[14] Moreover, TBT has been shown to induce neuronal death by glutamate excitotoxicity in cultured rat cortical neurons.[15] Although the use of TBT has already been restricted, butyltin compounds, including TBT, have been reported to be still present at concentrations between 50 and 400 nM in human blood.[16] However, the mechanism by which nanomolar levels of TBT cause cytotoxicity is not fully understood.

Glucose is the primary energy source for homeostasis. Glucose transport across the plasma membrane *via* a glucose transporter (GLUT) is a rate-limiting step in glucose metabolism.[17] AMP-activated protein kinase (AMPK), a serine threonine kinase, has been shown to regulate glucose uptake by facilitating the translocation of the GLUT to the membrane or by activation of transporter activity at the plasma membrane.[18,19] The fetal brain has been reported to rely on anaerobic glycolysis to meet its energy demands.[20] Thus, GLUT is considered essential in the early organogenesis period. GLUT1, a major subtype of GLUT in fetal tissue, has been shown to mediate organogenesis in rat embryos.[21] In addition, clinical data regarding human GLUT1 deficiency syndrome suggest that GLUT1 is necessary for human brain development.[22]

In the present study, we hypothesized a possible link between TBT toxicity and glucose metabolism. We found that

[a] *Division of Pharmacology, National Institute of Health Sciences, 1-18-1, Kamiyoga, Setagaya-ku 158-8501, Japan. E-mail: kanda@nihs.go.jp; Fax: +81-3-3700-9704; Tel: +81-3-3700-9704*

[b] *Department of Xenobiotic Metabolism and Molecular Toxicology, Graduate School of Biomedical and Health Sciences, Hiroshima University, Japan*

† Electronic supplementary information (ESI) available. See DOI: 10.1039/c3mt20268b

exposure to TBT reduced the amounts of glucose-6-phosphate and fructose-6-phosphate *via* a decrease in surface-bound GLUT1 in the human pluripotent embryonic carcinoma cell line NT2/D1. In addition, treatment with the potent AMPK activator, 5-aminoimidazole-4-carboxyamide ribonucleoside (AICAR), restored the inhibitory effect of TBT on both cell surface-bound GLUT1 levels and glucose uptake. We report here that the glycolytic pathway is a molecular target of nanomolar levels of TBT in human embryonic carcinoma cells.

Methods

Cell culture

NT2/D1 cells were obtained from the American Type Culture Collection. The cells were cultured in Dulbecco's modified Eagle's medium (DMEM; Sigma-Aldrich, St. Louis, MO, USA) supplemented with 10% fetal bovine serum (FBS; Biological Industries, Ashrat, Israel) and 0.05 mg mL^{-1} penicillin–streptomycin mixture (Life Technologies, Carlsbad, CA, USA) at 37 °C and 5% CO_2. For neural differentiation, all-trans retinoic acid (RA; Sigma-Aldrich) was added to the medium twice a week at a final concentration of 10 μM.

Cell proliferation assay

Cell viability was measured using the CellTiter 96 AQueous One Solution Cell Proliferation Assay (Promega, Madison, WI, USA), according to the manufacturer's instructions. Briefly, NT2/D1 cells were seeded into 96-well plates and exposed to different concentrations of TBT. After exposure to TBT, One Solution Reagent was added to each well, and the plate was incubated at 37 °C for another 2 h. Absorbance was measured at 490 nm using an iMark microplate reader (Bio-Rad, Hercules, CA, USA).

Glucose uptake assay

A glucose uptake assay was performed using a fluorescent glucose derivative, 2-[*N*-(7-nitrobenz-2-oxa-1,3-diazol-4-yl)amino]-2-deoxy-D-glucose (2-NBDG; Peptide Institute Inc., Osaka, Japan) by the previously reported procedure with slight modifications.[23] Briefly, NT2/D1 cells exposed to TBT were incubated with 2-NBDG (100 μM) for 2 h at 37 °C. The 2-NBDG uptake reaction was stopped by draining the incubation medium and washing the cells twice with ice-cold PBS. The incorporated 2-NBDG was measured using a Wallac1420ARVO fluoroscan (Perkin-Elmer, Waltham, MA, USA) with excitation at 488 nm and emission at 515 nm. The fluorescence intensities were normalized to the total protein content.

Hexokinase activity assay

Hexokinase activity was determined using a commercial Hexokinase Colorimetric Assay Kit (Biovision, Mountain View, CA, USA), according to the manufacturer's instructions.

AMPK activity assay

AMPK activity was determined using a commercial CycLex AMP Kinase Assay Kit (MBL International, Woburn, MA, USA), according to the manufacturer's instructions.

Determination of glucose-6-phosphate and fructose-6-phosphate

Intracellular metabolites were extracted and used for subsequent capillary electrophoresis time-of-flight mass spectrometry (CE-TOFMS) analysis, as described previously.[24] Glucose-6-phosphate and fructose-6-phosphate were determined using an Agilent CE capillary electrophoresis system (Agilent Technologies, Waldbronn, Germany) equipped with an Agilent G3250AA LC/MSD TOF system (Agilent Technologies, Palo Alto, CA), an Agilent 1100 series isocratic HPLC pump, a G1603A Agilent CE-MS adapter kit, and a G1607A Agilent CE-electrospray ionization 53-MS sprayer kit. For system control and data acquisition, G2201AA Agilent ChemStation software was used for CE, and Agilent TOF (Analyst QS) software was used for TOFMS.

Western blotting

Western blotting was performed as previously reported.[25] Briefly, the cells were lysed using Cell Lysis Buffer (Cell Signaling Technology, Danvers, MA, USA), and proteins were then separated by sodium dodecyl sulfate (SDS)-polyacrylamide gel electrophoresis and electrophoretically transferred to Immobilon-P membranes (Millipore, Billerica, MA, USA). The membranes were probed using primary antibodies (anti-GLUT1 polyclonal antibodies [1 : 200; Santa Cruz Biotechnology, Santa Cruz, CA, USA], anti-c-Myc polyclonal antibodies [1 : 1000; Sigma-Aldrich], anti-Flag monoclonal antibodies [1 : 1000; Sigma-Aldrich], and anti-β-actin monoclonal antibodies [1 : 1000; Sigma-Aldrich]). The membranes were then incubated with secondary antibodies against rabbit or mouse IgG conjugated with horseradish peroxidase (Cell Signaling Technology). The bands were visualized using an ECL Western Blotting Analysis System (GE Healthcare, Buckinghamshire, UK), and images were acquired using a LAS-3000 Imager (Fujifilm UK Ltd., Systems, Bedford, UK). The density of each band was quantified with ImageJ software (NIH, Bethesda, MD, USA).

Cell surface biotinylation

NT2/D1 cell surface proteins were biotinylated using a Cell Surface Protein Isolation Kit, according to the manufacturer's instructions (Pierce, Rockford, IL, USA). Briefly, cells were incubated with ice-cold phosphate-buffered saline (PBS; pH 7.4) containing Sulfo-NHS-SS-Biotin, with gentle rocking for 30 min at 4 °C. The biotinylated proteins were precipitated with streptavidin beads and eluted from the beads with SDS sample buffer. The proteins were analyzed by western blotting with anti-GLUT1 antibodies.

Immunohistochemistry

Cells, cultured on glass coverslips, were fixed in 4% paraformaldehyde in PBS (pH 7.4) for 15 min at room temperature. The fixed cells were incubated with anti-GLUT1 polyclonal antibodies (1 : 100; Santa Cruz) for 1 h at room temperature. Finally, they were incubated with Alexa488-conjugated secondary antibodies (1 : 200; Life Technologies) for 1 h at room temperature. The cells were enclosed in SlowFade (Life Technologies) and examined under a BIOREVO BZ-9000 fluorescent microscope (Keyence, Osaka, Japan).

Transfection

Cells were transiently transfected with Flag-tagged GLUT1 in pEF6 (a kind gift from Dr Rathmell) and c-Myc-tagged constitutively active-AMPK-α1 (T172D) or c-Myc-tagged dominant-negative-AMPK-α1 (K45R) in pcDNA3 (a kind gift from Dr Carling) using the FuGene HD Transfection Reagent (Promega), according to the manufacturer's protocol. After 48 h incubation, the transfectants were cultured with 12.5 μg mL^{-1} blasticidin or 0.5 mg mL^{-1} G418.

Real-time PCR

After total RNA was isolated from NT2/D1 cells using TRIzol (Life Technologies), quantitative real-time reverse transcription (RT)-PCR with a QuantiTect SYBR Green RT-PCR Kit (QIAGEN, Valencia, CA, USA) was performed using an ABI PRISM 7900HT sequence detection system (Applied Biosystems, Foster City, CA, USA), as previously reported.[26] The relative changes in the amounts of transcripts in each sample were normalized using ribosomal protein L13 (RPL13) mRNA levels. The sequences of the primers used for real-time PCR analysis are as follows: GLUT1 (forward, 5′-CCAGCTGCCATTGCCGTT-3′; reverse, 5′-GACGTAGGGACCACACAGTTGC-3′), GLUT2 (forward, 5′-CACACAAGACCTGGAATTGACA-3′; reverse, 5′-CGGTCATCCAGTGGAACAC-3′), GLUT3 (forward, 5′-CAATGCTCCTGAGAAGATCATAA-3′; reverse, 5′-AAAGCGGTTGACGAAGAGT-3′), GLUT4 (forward, 5′-CTGGGCCTCACAGTGCTAC-3′; reverse, 5′-GTCAGGCGCTTCAGACTCTT-3′), nestin (forward, 5′-GGCAGCGTTGGAACAGAGGT-3′; reverse, 5′-CATCTTGAGGTGCGCCAGCT-3′), NeuroD (forward, 5′-GGAAACGAACCCACTGTGCT-3′; reverse, 5′-GCCACACCAAATTCGTGGTG-3′), Math1 (forward, 5′-GTCCGAGCTGCTACAAACG-3′; reverse, 5′-GTGGTGGTGGTCGCTTTT-3′), MAP2 (forward, 5′-CCAATGGATTCCCATACAGG-3′; reverse, 5′-CTGCTACAGCCTCAGCAGTG-3′), RPL13 (forward, 5′-CATCGTGGCTAAACAGGTACTG-3′; reverse, 5′-GCACGACCTTGAGGGCAGCC-3′).

Materials

TBT was obtained from Tokyo Chemical Industry (Tokyo, Japan). Tin acetate (TA), AICAR, and rosiglitazone were obtained from Sigma-Aldrich. All other reagents were of analytical grade and obtained from commercial sources.

Statistical analysis

All data were presented as mean ± S.D. ANOVA followed by a *post hoc* Tukey test was used to analyze data in Fig. 1–4. Unpaired Student's *t* test was used to analyze data in Fig. 5. A *p* value of less than 0.05 was considered significant.

Results

To examine the effect of TBT on the proliferation of human NT2/D1 embryonic carcinoma cells, we exposed the cells to different concentrations of TBT for 24 h and measured cell viability by MTT assay. Treatment with TBT reduced cell viability in a dose-dependent manner (Fig. 1A; 0.03–0.3 μM). We observed that almost all cells were detached from the culture dish at TBT concentrations of 300 nM and above. In contrast, the less toxic TA had little effect at any concentration (Fig. 1A–e). We performed time-course experiments with 100 nM TBT, and determined the cell number. Exposure to

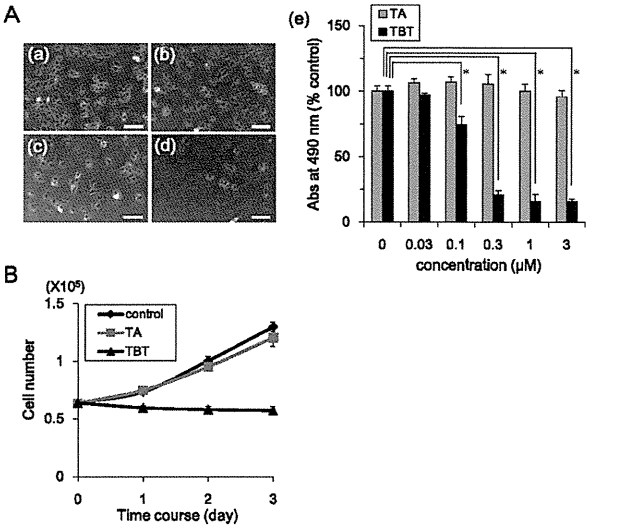

Fig. 1 Effect of TBT exposure on cell proliferation in NT2/D1 cells. (A) NT2/D1 cells were seeded into 96-well plates and exposed to TBT at different concentrations for 24 h. (a–d) Phase-contrast photomicrographs of NT2/D1 cells exposed to TBT at 0, 0.03, 0.1, or 0.3 μM (Bar = 100 μm). (e) Cell viability in the presence of TBT or TA was examined using the CellTiter 96 AQueous One Solution Cell Proliferation Assay. (B) NT2/D1 cells (6×10^5 cells) were seeded into 100 mm dishes and exposed to 100 nM TBT. After 24, 48, and 72 h, cell count was determined using a hemocytometer. *$P < 0.05$.

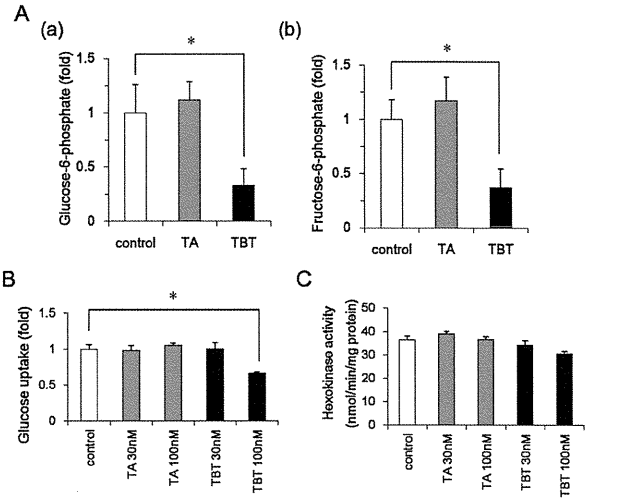

Fig. 2 Effect of TBT exposure on glycolytic systems in NT2/D1 cells. (A) After 24 h exposure to 100 nM TBT or TA, glucose 6-phosphate (a) and fructose 6-phosphate (b) levels were determined using CE-TOFMS. (B) After exposure to TBT or TA (30, 100 nM) for 24 h, glucose uptake assay was performed using a fluorescent glucose analog 2-NBDG. The fluorescence intensities of incorporated 2-NBDG were normalized to total cellular protein content. (C) After exposure to TBT or TA (30, 100 nM) for 24 h, hexokinase activity was measured using a commercial assay kit. *$P < 0.05$.

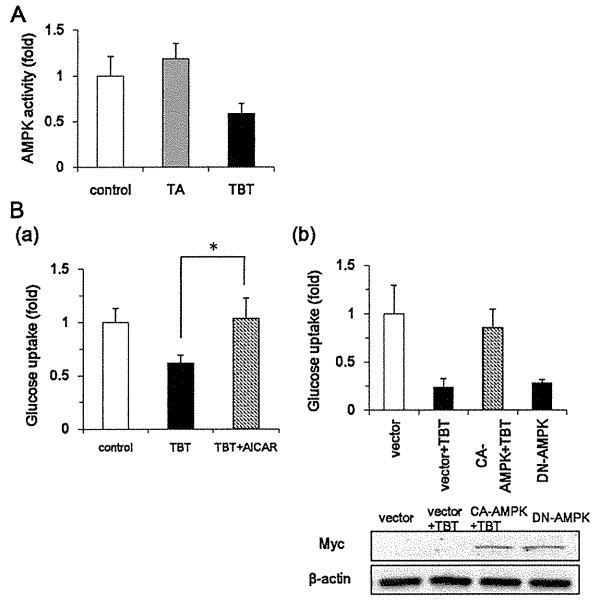

Fig. 3 Effect of AMPK on glucose uptake in NT2/D1 cells. (A) NT2/D1 cells were exposed to TBT or TA at 100 nM for 24 h. AICAR (0.5 mM) treatment was performed for 3 h. AMPK activity in the lysed cells was determined using a commercial assay kit. (B) NT2/D1 cells were exposed to TBT in the presence of 0.5 mM AICAR. (C) After overexpression of constitutively active (CA) mutants of AMPK, NT2/D1 cells were exposed to 100 nM TBT for 24 h, and glucose uptake assay was performed. After overexpression of dominant-negative (DN) mutants of AMPK, basal glucose uptake was tested. A glucose uptake assay was performed using the fluorescent glucose analog 2-NBDG. The fluorescence intensities of incorporated 2-NBDG were normalized to total cellular protein content. $^*P < 0.05$.

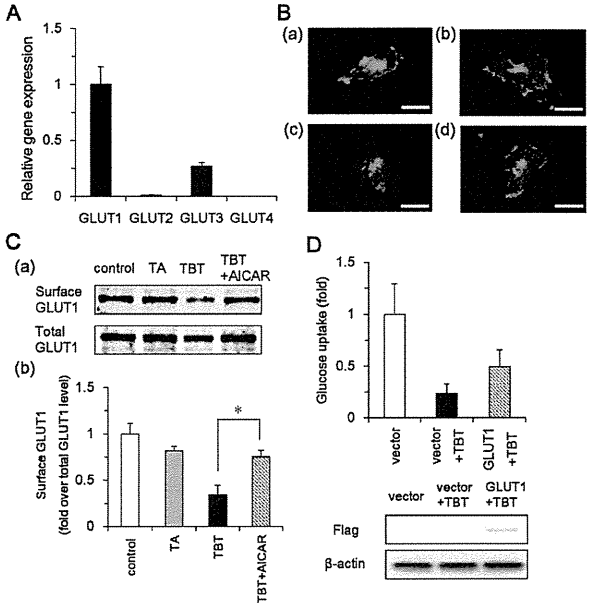

Fig. 4 Effect of TBT exposure on GLUT1 localization in NT2/D1 cells. (A) Expression of GLUT family by real-time PCR in NT2/D1 cells. Relative changes were determined by normalizing to RPL13. (B) After exposure to 100 nM TBT for 24 h, NT2/D1 cells were immunostained with anti-GLUT1 polyclonal antibodies. (a) Control, (b) 100 nM TA, (c) 100 nM TBT, and (d) 100 nM TBT + 0.5 mM AICAR. (Bar = 25 μm). (C) (a) NT2/D1 cell surface proteins were biotinylated using Sulfo-NHS-SS-Biotin, and then lysed. After precipitation with streptavidin beads, biotinylated proteins were analyzed by western blotting using anti-GLUT1 antibodies. Total GLUT1 protein was detected in cell lysate. (b) The relative density of bands was quantified with ImageJ software. Cell surface GLUT1 levels were normalized to total GLUT1 levels. (D) After overexpression of GLUT1, NT2/D1 cells were exposed to 100 nM TBT for 24 h, and glucose uptake assay was performed using the fluorescent glucose analog 2-NBDG. The fluorescence intensities of incorporated 2-NBDG were normalized to total cellular protein content. $^*P < 0.05$.

TBT suppressed the growth curve, but the total cell number did not alter throughout the time-course experiment (Fig. 1B). These data suggest that exposure to 100 nM TBT induced growth arrest in the cells without causing cell death.

Glucose provides metabolic energy for cell growth and it is incorporated by glucose transporters.[17] To examine the mechanism by which TBT induces growth arrest at low concentrations, we determined the glucose-6-phosphate, a major metabolite in glycolysis. We found that exposure to 100 nM TBT reduced the amount of glucose-6-phosphate (Fig. 2A). Fructose-6-phosphate, which is produced by isomerization of glucose 6-phosphate, also reduced by TBT. To check whether the decrease in glucose-6-phosphate is induced by inhibition of glucose transport, we examined the activity of glucose uptake by using 2-NBDG, a fluorescently labeled 2-deoxyglucose. Similar to the cell growth, glucose uptake was significantly inhibited by 100 nM TBT, not by 30 nM TBT (Fig. 2B). TA had little effect on glucose uptake. To examine whether the inhibition is regulated by transcription, we tested the effect of short-term exposure. Exposure to TBT for 1 h suppressed glucose uptake (Fig. S1, ESI†), suggesting that gene expression is not involved in the effect of TBT. Since TBT has been shown to activate transcriptional activity of peroxisome proliferator-activated receptor γ (PPARγ),[27,28] we tested the effect of the PPARγ agonist rosiglitazone on the glucose uptake. Treatment with rosiglitazone increased glucose uptake (Fig. S2, ESI†), suggesting that PPARγ is not involved in TBT-induced inhibition of glucose uptake. Furthermore, we examined the activity of hexokinase, which catalyzes the phosphorylation of glucose into glucose-6-phosphate. As shown in Fig. 2C, hexokinase activity was not significantly altered by TBT. Exposure to TA also produced similar results. These data suggest that TBT exposure decreases the amount of glycolytic metabolites *via* inhibition of glucose transport.

AMP-activated protein kinase (AMPK) is known to regulate the translocation of a glucose transporter (GLUT) to the plasma membrane.[29] We examined whether AMPK is involved in the inhibition of glycolytic systems by TBT exposure. Exposure to 100 nM TBT reduced AMPK activity (Fig. 3A). In contrast, TA had little effect on AMPK. In addition, treatment with AICAR (a potent AMPK activator) recovered the inhibitory effect of TBT on glucose uptake (Fig. 3B). To confirm the effect of AICAR, we examined the effect of constitutively active (CA) mutants of AMPK. Similar to the treatment with AICAR, overexpression of CA-AMPK recovered the inhibitory effect of TBT on glucose uptake. Overexpression of dominant-negative mutants of AMPK reduced the basal level of glucose uptake, suggesting that

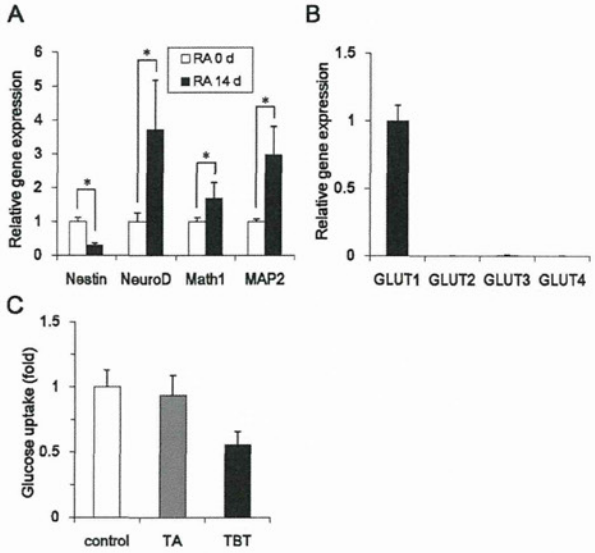

Fig. 5 Effect of neuronal induction on glucose uptake under TBT exposure in NT2/D1 cells. (A) To induce neuronal differentiation, NT2/D1 cells were treated with 10 μM RA for 14 days. The relative expression of neuronal markers (NeuroD, Math1, and MAP2) and a marker of undifferentiation (nestin) were measured by real-time-PCR. The relative changes were normalized to RPL13. (B) Expressions of members of the GLUT family were measured by real-time PCR in differentiated NT2/D1 cells. Relative changes were determined by normalizing to RPL13. (C) After exposure to 100 nM TBT for 24 h, glucose uptake was measured in differentiated cells. The fluorescence intensities of intracellularly incorporated 2-NBDG were measured and normalized to the total cellular protein levels. $^{*}P < 0.05$.

glucose uptake is AMPK-dependent in NT2/D1 cells. Taken together, these data suggest that TBT exposure suppresses glucose uptake through the inhibition of AMPK activity.

We next examined the mechanism by which AMPK regulates glucose uptake in NT2/D1 cells. Real-time PCR analysis showed that GLUT1 was a major subtype in NT2/D1 cells (Fig. 4A). Since TBT exposure did not affect gene expression of GLUT1 (data not shown), we examined GLUT1 localization by immunohistochemistry. Expression of GLUT1 was observed at the plasma membrane and in the intracellular segment (Fig. 4B). Exposure with TBT reduced the cell surface expression of GLUT1. Treatment with AICAR recovered the inhibitory effect of TBT. To confirm these observations using microscopy, we labeled cell surface-bound GLUT1 by biotinylation of cell surface proteins (Fig. 4C). Using this approach, we determined that TBT exposure reduced the amount of cell surface-bound GLUT1. AICAR reversed this inhibitory effect of TBT. Furthermore, overexpression of GLUT1 partially recovered the TBT-induced inhibition of glucose uptake (Fig. 4D). These data suggest that TBT inhibits glucose uptake mediated by cell surface translocation of GLUT1, a process dependent on AMPK.

To examine whether the effect of TBT was selective for embryonic cells, we used NT2/D1 cells differentiated by retinoic acid.[30] Real-time PCR analysis revealed that RA-treated NT2/D1 cells showed upregulated expression of markers of differentiation (NeuroD, Math1, MAP2) and downregulated expression of a marker of undifferentiation (nestin), confirming the induction of differentiation (Fig. 5A). Real-time PCR confirmed that GLUT1 is a major subtype in the differentiated NT2/D1 cells (Fig. 5B). Furthermore, exposure to 100 nM TBT also reduced glucose uptake in differentiated NT2/D1 cells. In contrast, TA had little effect (Fig. 5C). These data suggest that TBT suppresses glucose uptake in both undifferentiated and differentiated cells.

Discussion

In the present study, we showed that the glycolytic pathway is a novel target of TBT toxicity in human embryonic carcinoma cells. We showed that TBT suppresses AMPK-dependent glucose uptake, and thereby, the amount of glucose-6-phosphate. The inhibitory effects of TBT on glycolytic systems would lead to growth arrest in the cells. Fig. 6 shows a proposed model of TBT-induced toxicity, based on the data observed in our study.

Our studies showed that treatment with 1 μM TBT resulted in the death of human embryonic carcinoma cells (Fig. 1). Consistent with these observations, previous studies have shown that micromolar levels of TBT induce apoptosis in various cells such as human amnion cells,[31] hepatocytes,[32] and neutrophils.[33] In contrast, exposure to 100 nM TBT resulted in neither growth arrest nor cell death. Therefore, we focused on intracellular metabolites as potential mediators of TBT-induced growth arrest. We found that exposure to nanomolar levels of TBT affects the intracellular metabolic balance and decreases the amount of glucose metabolites (Fig. 2). A previous report showed that the organotin compounds such as TBT might be present in human blood at nanomolar levels.[16] Glucose metabolism analysis revealed novel toxic mechanisms

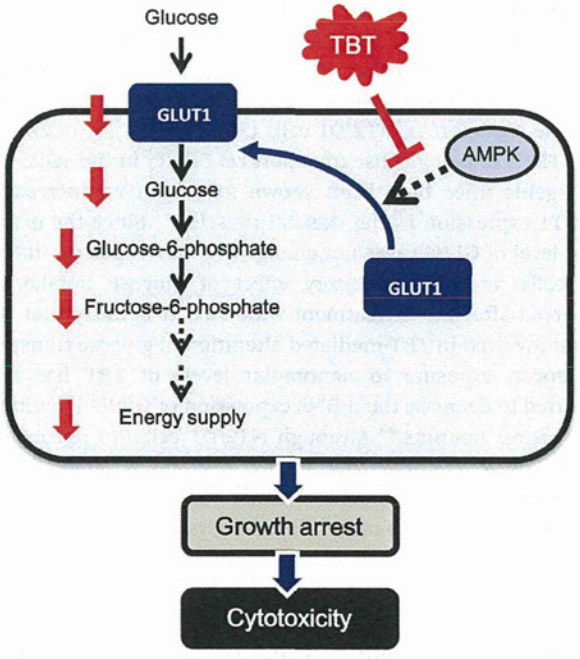

Fig. 6 Proposed model of TBT toxicity in human embryonic carcinoma cells.

for the toxicity of nanomolar levels of TBT. Thus, the glycolytic pathway might account for the unknown toxic mechanism induced by heavy metal exposure.

Our data suggest that the target molecule of TBT toxicity is GLUT1, a major subtype of GLUT in NT2/D1 cells (Fig. 4). Since the expression of GLUT1 is observed in a broad range of cell types, the toxicity of TBT may also be observed in other cells. For example, we showed that TBT reduces glucose uptake in differentiated NT2/D1 cells, which express GLUT1 (Fig. 5). Thus, it is possible that TBT induces toxicity in mature neurons *via* inhibition of GLUT function.

We showed that TBT decreases AMPK activity, one of the GLUT regulators, in NT2/D1 cells (Fig. 3). In addition, overexpression of AMPK or the AMPK activator restored the glucose uptake, confirming that AMPK is a possible target of TBT. In contrast, 500 nM TBT has been shown to increase AMPK phosphorylation in rat cortical neurons.[34] This discrepancy might be due to the concentration of TBT or different types of cells.

Several studies suggest that TBT directly interacts with target enzymes. TBT at a concentration of 10–100 nM has been shown to act as an agonist of PPARγ and the retinoid X receptor (RXR) because of its higher binding affinity compared to intrinsic ligands. Other studies reported that micromolar concentrations of TBT inhibit F1F0 ATP synthase and 11β-hydroxysteroid dehydrogenase by direct interaction.[35,36] Therefore, TBT can bind to multiple targets with broad specificity. It is possible that TBT also interacts with AMPK. On the other hand, calmodulin-dependent protein kinase II (CaMK II) and serine–threonine liver kinase B1 (LKB1) have been shown to phosphorylate AMPK and cause subsequent activation of glucose transport.[29] Furthermore, there may be an additional signaling molecule between TBT and AMPK. It remains to be elucidated how TBT regulates AMPK in embryonic carcinoma cells.

Nanomolar levels of TBT may interact with several targets in other types of cells, such as PPARγ, RXR, and α-amino-3-hydroxy-5-methylisoxazole-4-propionic acid (AMPA) receptors 2 (GluR2). Since rosiglitazone, a PPARγ agonist, increased glucose transport in NT2/D1 cells (Fig. S2, ESI†), it is unlikely that TBT inhibits glucose transport *via* PPARγ in the cells. RXR transgenic mice have been shown to exhibit an increase in GLUT1 expression in the skeletal muscles.[37] Since the expression level of GLUT1 was not changed by TBT exposure in NT2/D1 cells and the inhibitory effect of glucose uptake was observed after a 1 h treatment with TBT, it is likely that RXR is not involved in TBT-mediated alteration of glucose transport. Moreover, exposure to nanomolar levels of TBT has been reported to decrease the mRNA expression of GluR2 in cultured rat cortical neurons.[38] Although NT2/D1 cells do not express GluR2, it is possible that GluR2 may be a target in the differentiated NT2/D1 cells. Further studies are required to examine these targets other than the glycolytic pathway.

Conclusions

We found that exposure to nanomolar levels of TBT mainly targets the glycolytic systems in human embryonic carcinoma cells. Thus, glycolytic systems may be a good target for previously unknown mechanisms of toxicity induced by metal exposure at nanomolar levels.

Conflict of interest

The authors declare that there are no conflicts of interest.

List of abbreviations

AMPK	AMP-activated protein kinase
GLUT	glucose transporter
RA	all-trans retinoic acid
PPARγ	peroxisome proliferator-activated receptor γ
TA	tin acetate
TBT	tributyltin

Acknowledgements

We would like to thank Dr Rathmell and Dr Carling for providing the materials. This study was supported in part by a Health and Labour Sciences Research Grant from the Ministry of Health, Labour and Welfare, Japan (Y. Ka.), a grant from the Program for Promotion of Fundamental Studies in Health Sciences of the National Institute of Biomedical Innovation (NIBIO) (No. 09-02 to Y. Ka.), Grants-in-Aid for Scientific Research (No. 23590322 to Y. Ka. and No. 23310047 to Y. Ko.) from the Japan Society for the Promotion of Science, and a grant from the Smoking Research Foundation (Y. Ka.).

References

1 H. L. Needleman, C. Gunnoe, A. Leviton, R. Reed, H. Peresie, C. Maher and P. Barrett, Deficits in psychologic and classroom performance of children with elevated dentine lead levels, *N. Engl. J. Med.*, 1979, **300**, 689–695.
2 G. Winneke, Developmental aspects of environmental neurotoxicology: lessons from lead and polychlorinated biphenyls, *J. Neurol. Sci.*, 2011, **308**, 9–15.
3 L. G. Costa, M. Aschne, A. Vitalone, T. Syversen and O. P. Soldin, Developmental neuropathology of environmental agents, *Annu. Rev. Pharmacol. Toxicol.*, 2004, **44**, 87–110.
4 J. Dobbing, *Vulnerable periods in developing brain*, in *Appl. Neurochem.*, ed. A. N. Davison and J. Dobbing, Davis, Philadelphia, 1968, pp. 287–316.
5 P. M. Rodier, Developing brain as a target of toxicity, *Environ. Health Perspect.*, 1995, **103**(suppl 6), 73–76.
6 D. Rice and S. Barone Jr, Critical periods of vulnerability for the developing nervous system: evidence from humans and animal models, *Environ. Health Perspect.*, 2000, **108**(suppl 3), 511–533.
7 H. Asakawa, M. Tsunoda, T. Kaido, M. Hosokawa, C. Sugaya, Y. Inoue, Y. Kudo, T. Satoh, H. Katagiri, H. Akita, M. Saji, M. Wakasa, T. Negishi, T. Tashiro and Y. Aizawa, Enhanced

inhibitory effects of TBT chloride on the development of F1 rats, *Arch. Environ. Contam. Toxicol.*, 2010, **58**, 1065–1073.
8 S. Gómez-Ruiz, G. N. Kaluderović, S. Prashar, E. Hey-Hawkins, A. Erić, Z. Zizak and Z. D. Juranić, Study of the cytotoxic activity of di and triphenyltin(IV) carboxylate complexes, *J. Inorg. Biochem.*, 2008, **102**, 2087–2096.
9 L. Rocamora-Reverte, E. Carrasco-García, J. Ceballos-Torres, S. Prashar, G. N. Kaluđerović, J. A. Ferragut and S. Gómez-Ruiz, Study of the anticancer properties of tin(IV) carboxylate complexes on a panel of human tumor cell lines, *ChemMedChem*, 2012, **7**, 301–310.
10 A. González, E. Gómez, A. Cortés-Lozada, S. Hernández, T. Ramírez-Apan and A. Nieto-Camacho, Heptacoordinate tin(IV) compounds derived from pyridine Schiffbases: synthesis, characterization, *in vitro* cytotoxicity, anti-inflammatory and antioxidant activity, *Chem. Pharm. Bull.*, 2009, **57**, 5–15.
11 Y. Kotake, Molecular mechanisms of environmental organotin toxicity in mammals, *Biol. Pharm. Bull.*, 2012, **35**, 1876–1880.
12 T. Noda, S. Morita, T. Yamano, M. Shimizu, T. Nakamura, M. Saitoh and A. Yamada, Teratogenicity study of tri-*n*-butyltin acetate in rats by oral administration, *Toxicol. Lett.*, 1991, **55**, 109–115.
13 A. T. Gardlund, T. Archer, K. Danielsen, B. Danielsson, A. Frederiksson, N. G. Lindquist, H. Lindstrom and J. Luthman, Effects of prenatal exposure to tributyltin and trihexyltin on behavior in rats, *Neurotoxicol. Teratol.*, 1991, **13**, 99–105.
14 Q. Li, M. Osada, K. Takahashi, T. Matsutani and K. Mori, Accumulation and depuration of tributyltin oxide and its effect on the fertilization and embryonic development in the pacific oyster, *Crassostrea gigas*, *Bull. Environ. Contam. Toxicol.*, 1997, **58**, 489–496.
15 Y. Nakatsu, Y. Kotake, K. Komasaka, H. Hakozaki, R. Taguchi, T. Kume, A. Akaike and S. Ohta, Glutamate excitotoxicity is involved in cell death caused by tributyltin in cultured rat cortical neurons, *Toxicol. Sci.*, 2006, **89**, 235–242.
16 M. M. Whalen, B. G. Loganathan and K. Kannan, Immunotoxicity of environmentally relevant concentrations of butyltins on human natural killer cells *in vitro*, *Environ. Res. Lett.*, 1999, **81**, 108–116.
17 L. Pellerin, Food for thought: the importance of glucose and other energy substrates for sustaining brain function under varying levels of activity, *Diabetes Metab.*, 2010, **36**, S59–S63.
18 K. Barnes, J. C. Ingram, O. H. Porras, L. F. Barros, E. R. Hudson, L. G. Fryer, F. Foufelle, D. Carling, D. G. Hardie and S. A. Baldwin, Activation of GLUT1 by metabolic and osmotic stress: potential involvement of AMP-activated protein kinase (AMPK), *J. Cell Sci.*, 2002, **115**, 2433–2442.
19 M. Jing, V. K. Cheruvu and F. Ismail-Beigi, Stimulation of glucose transport in response to activation of distinct AMPK signaling pathways, *Am. J. Physiol.: Cell Physiol.*, 2008, **295**, C1071–C1082.
20 B. Kunievsky, J. Pretsky and E. Yavin, Transient rise of glucose uptake in the fetal rat brain after brief episodes of intrauterine ischemia, *Dev. Neurosci.*, 1994, **16**, 313–320.
21 K. Matsumoto, S. Akazawa, M. Ishibashi, R. A. Trocino, H. Matsuo, H. Yamasaki, Y. Yamaguchi, S. Nagamatsu and S. Nagataki, Abundant expression of GLUT1 and GLUT3 in rat embryo during the early organogenesis period, *Biochem. Biophys. Res. Commun.*, 1995, **209**, 95–102.
22 P. J. Jensen, J. D. Gitlin and M. O. Carayannopoulos, GLUT1 deficiency links nutrient availability and apoptosis during embryonic development, *J. Biol. Chem.*, 2006, **281**, 13382–13387.
23 Y. Kanda and Y. Watanabe, Thrombin-induced glucose transport *via* Src-p38 MAPK pathway in vascular smooth muscle cells, *Br. J. Pharmacol.*, 2005, **146**, 60–67.
24 T. Soga, Y. Ueno, H. Naraoka, Y. Ohashi, M. Tomita and T. Nishioka, Simultaneous determination of anionic intermediates for *Bacillus subtilis* metabolic pathways by capillary electrophoresis electrospray ionization mass spectrometry, *Anal. Chem.*, 2002, **74**, 2233–2239.
25 Y. Kanda and Y. Watanabe, Adrenaline increases glucose transport *via* a Rap1-p38MAPK pathway in rat vascular smooth muscle cells, *Br. J. Pharmacol.*, 2007, **151**, 476–482.
26 N. Hiarta, Y. Sekinoa and Y. Kanda, Nicotine increases cancer stem cell population in MCF-7 cells, *Biochem. Biophys. Res. Commun.*, 2010, **403**, 138–143.
27 T. Kanayama, N. Kobayashi, S. Mamiya, T. Nakanishi and J. Nishikawa, Organotin compounds promote adipocyte differentiation as agonists of the peroxisome proliferator-activated receptor gamma/retinoid X receptor pathway, *Mol. Pharmacol.*, 2005, **67**, 766–774.
28 F. Grün, H. Watanabe, Z. Zamanian, L. Maeda, K. Arima, R. Cubacha, D. M. Gardiner, J. Kanno, T. Iguchi and B. Blumberg, Endocrine-disrupting organotin compounds are potent inducers of adipogenesis in vertebrates, *Mol. Endocrinol.*, 2006, **20**, 2141–2155.
29 D. G. Hardie, F. A. Ross and S. A. Hawley, AMPK: a nutrient and energy sensor that maintains energy homeostasis, *Nat. Rev. Mol. Cell Biol.*, 2012, **13**, 251–262.
30 S. J. Pleasure, C. Page and V. M. Lee, Pure, postmitotic, polarized human neurons derived from NTera 2 cells provide a system for expressing exogenous proteins in terminally differentiated neurons, *J. Neurosci.*, 1992, **12**, 1802–1815.
31 X. Zhu, M. Xing, J. Lou, X. Wang, W. Fu and L. Xu, Apoptotic related biochemical changes in human amnion cells induced by tributyltin, *Toxicology*, 2007, **230**, 45–52.
32 M. Grondin, M. Marion, F. Denizeau and D. A. Averill-Bate, Tributyltin induces apoptotic signaling in hepatocytes through pathways involving the endoplasmic reticulum and mitochondria, *Toxicol. Appl. Pharmacol.*, 2007, **222**, 57–68.
33 V. Lavastre and D. Girard, Tributyltin induces human neutrophil apoptosis and selective degradation of cytoskeletal proteins by caspases, *J. Toxicol. Environ. Health, Part A*, 2002, **65**, 1013–1024.

34 Y. Nakatsu, Y. Kotake, A. Hino and S. Ohta, Activation of AMP-activated protein kinase by tributyltin induces neuronal cell death, *Toxicol. Appl. Pharmacol.*, 2008, **230**, 358–363.
35 C. von Ballmoos, J. Brunner and P. Dimroth, The ion channel of F-ATP synthase is the target of toxic organotin compounds, *Proc. Natl. Acad. Sci. U. S. A.*, 2004, **101**, 11239–11244.
36 A. G. Atanasov, L. G. Nashev, S. Tam, M. E. Baker and A. Odermatt, Organotins disrupt the 11β-hydroxysteroid dehydrogenase type 2-dependent local inactivation of glucocorticoids, *Environ. Health Perspect.*, 2005, **113**, 1600–1606.
37 S. Sugita, Y. Kamei, F. Akaike, T. Suganami, S. Kanai, M. Hattori, Y. Manabe, N. Fujii, T. Takai-Igarashi, M. Tadaishi, J. Oka, H. Aburatani, T. Yamada, H. Katagiri, S. Kakehi, Y. Tamura, H. Kubo, K. N. S. Miura, O. Ezaki and Y. Ogawa, Increased systemic glucose tolerance with increased muscle glucose uptake in transgenic mice overexpressing RXRγ in skeletal muscle, *PLoS One*, **6**, e20467.
38 Y. Nakatsu, Y. Kotake Y, T. Takishit and S. Ohta, Long-term exposure to endogenous levels of tributyltin decreases GluR2 expression and increases neuronal vulnerability to glutamate, *Toxicol. Appl. Pharmacol.*, 2009, **240**, 292–298.

